

Wu, Qiong, Role of  $\Delta$ FosB in nucleus of the solitary tract (NTS) in cardiovascular adaptations to chronic intermittent hypoxia (CIH) in rats. Doctor of Philosophy (Biomedical Sciences), July 2015, 121 pp. , 16 figures, bibliograph, 146 references.

Chronic intermittent hypoxia (CIH) rodent model is widely utilized to study obstructive sleep apnea (OSA) associated disease such as hypertension. Arterial chemoreceptor is activated by CIH, and leads to increased sympathetic nerve discharge, resulting in elevated arterial pressure. The central neuronal mechanisms of CIH induced hypertension are barely understood. The nucleus of the solitary tract (NTS) receives the first synaptic inputs from arterial chemoreceptor afferents. Transcription factor  $\Delta$ FosB is increased in the NTS after a 7 day-CIH exposure. We hypothesize that NTS  $\Delta$ FosB could mediate neuronal plasticity, contribute to CIH induced hypertension.

Three specific aims were addressed. Aim 1: To determine the relationship between NTS  $\Delta$ FosB and CIH hypertension. Viral constructs were delivered into NTS to functionally block  $\Delta$ FosB ( $\Delta$ JunD group). Mean arterial pressure (MAP) was measured in day time when rats were exposed to intermittent hypoxia and night time when they were in normoxia. The increase in MAP observed in  $\Delta$ JunD and sham groups during day time was dampened in  $\Delta$ JunD group during night time, indicating the contribution of  $\Delta$ FosB to the sustained component of CIH associated hypertension. Aim 2: To determine the time-course of induction of  $\Delta$ FosB immunoreactive NTS neurons during CIH exposure. Rats were separated into normoxia, 1 day, 3, 5, 7 days CIH, and 1 day, 3, 7 days recovery after 7 days CIH groups.  $\Delta$ FosB immunoreactivity increased within 1

day CIH, and maintained this elevation throughout 7 days of CIH. 1 day recovery was sufficient to reduce  $\Delta$ FosB immunoreactivity to normoxia level. Therefore,  $\Delta$ FosB under CIH develops rapidly. Aim 3: To determine the function of  $\Delta$ FosB in glutamatergic transmission after CIH. Miniature excitatory post-synaptic current (mEPSC) properties of NTS neurons of rats exposed to either different days of CIH or room air were compared. CIH increased mEPSC amplitude but not frequency, suggesting a post-synaptic site of effect. Additionally, functional blockade of NTS  $\Delta$ FosB with  $\Delta$ JunD decreased mEPSC amplitude back to normoxia level. Finally, overexpression of NTS  $\Delta$ FosB increased mEPSC amplitude to similar levels as CIH. These results suggest that  $\Delta$ FosB in NTS neurons mediates molecular adaptations which might play an important role in CIH associated hypertension.

**ROLE OF  $\Delta$ FOSB IN NUCLEUS OF THE SOLITARY TRACT (NTS) IN  
CARDIOVASCULAR ADAPTATIONS TO CHRONIC INTERMITTENT HYPOXIA  
(CIH) IN RATS**

Qiong Wu, M.B.B.S

APPROVED:

---

Major Professor

---

Committee Member

---

Committee Member

---

Committee Member

---

University Member

---

Chair, Department of Integrative Physiology & Anatomy

---

Dean, Graduate School of Biomedical Sciences

**ROLE OF  $\Delta$ FOSB IN NUCLEUS OF THE SOLITARY TRACT (NTS) IN  
CARDIOVASCULAR ADAPTATIONS TO CHRONIC INTERMITTENT HYPOXIA  
(CIH) IN RATS**

DISSERTATION

Presented to the Graduate Council of the

University of North Texas Health Science Center at Fort Worth

In Partial Fulfillment of the Requirements

For the Degree of

DOCTOR OF PHILOSOPHY

By

Qiong Wu, M.B.B.S

Fort Worth, Texas

July 2015

## **ACKNOWLEDGEMENTS**

I would never been able to complete this dissertation without the guidance of my major professor, committee members, and help from friends as well as support from my family.

I would like to express my deepest gratitude to Dr. Steve Mifflin, who as my mentor, gave me limitless advice and full support. It is his intelligent and patient advising that raised me up to be an independent researcher in the future. I would like to extend my appreciation to my committee members: Drs. Tom Cunningham, Ann Schreihofner, Rong Ma, Michael Gatch, for their valuable suggestions and constructive criticism. I would particularly like to thank Dr. Yun Fan, who taught me the whole cell patch clamping technique. I also want to thank all my lab members: Mayurika, Kenta, Chandra, Michelle, Joel and Arthur, for their friendship and cooperation. I thank Susan Rogers, Lisa Marquez, Melissa Henson and Glenda Hawkins for their taking care of orderings, room schedule, reimbursement and other administrative details. I would like to thank all the faculty, staff and students in the Department of Physiology and Anatomy at the University of North Texas Health Science Center for providing such a wonderful environment to me to pursue my graduate career goals. Because of them, our department is like a warm family, and I did not feel lonely so far away from my homeland.

I am very indebted and thankful to my parents Jianbin Wu and Yunfeng Lu for their endless love and unconditional support. I dedicate this dissertation to them. They are always my source of joy, my love and hope.

I would gratefully acknowledge the financial support of National institute of Health HL-088052 and American Heart Association Pre-doctoral fellowship 13PRE16970013.

## **ABBREVIATIONS**

**AAV** Adeno-associated virus

**AP-1** Activator Protein-1

**AMPA**  $\alpha$ -amino-3-hydroxy-5-methyl-4-isoxazolepropionate

**CIH** Chronic intermittent hypoxia

**CNS** Central nervous system

**CPAP** Continuous positive airway pressure

**CR** Chemoreceptor

**CVLM** Caudal ventro-lateral medulla

**DBH** Dopamine beta hydroxylase

**DiA** 1,1'-dilinoleyl-3,3',3' tetramethylindocarbocyanine, 4-chlorobenzenesulphonate

**EAA** Excitatory amino acid

**GFP** Green fluorescent protein

**HR** Heart rate

**HPA** Hypothalamo-pituitary adrenal

**IML** Intermediolateral column

**MAP** Mean arterial pressure

**MnPO** Median pre-optic nucleus

**mEPSC** miniature excitatory postsynaptic current

**NMDA** N-methyl D-aspartate

**NTS** Nucleus of the solitary tract

**OSA** Obstructive sleep apnea

**PVN** Paraventricular nucleus

**RF** Respiratory frequency

**RVLM** Rostral ventro-lateral medulla

**SNA** Sympathetic nerve activity

**SND** Sympathetic nerve discharge

**TH** Tyrosine hydroxylase

## **PUBLICATIONS**

**Wu Q**, Mifflin SW. Transcription factor  $\Delta$ FosB enhances glutamatergic transmission in NTS following chronic exposures to intermittent hypoxia. (Submitted to **Am J Physiol Regul Integr Comp Physiol**, under revision)

**Wu Q**, Cunningham JT, Mifflin SW.  $\Delta$ FosB in the nucleus of the solitary tract contributes to persistent increase in mean arterial pressure during exposure to chronic intermittent hypoxia. (To be submitted)

**Wu Q**, Yun Fan, Mifflin SW. Corticosterone slowly enhances miniature excitatory postsynaptic current amplitude in NTS arterial chemoreceptor second order neurons. (In preparation)

## ABSTRACTS AND PRESENTATIONS

### **PUBLISHED ABSTRACTS**

Batliwala YS, **Wu Q**, Yamamoto K, Mifflin SW. Central nuclei activated during long-term facilitation of blood pressure following acute exposures to intermittent hypoxia. Research Appreciation Day, UNT Health Science Center, 2015.

**Wu Q**, Mifflin SW. Time course of changes in glutamatergic transmission within the nucleus of the solitary tract during chronic intermittent hypoxia exposure and the role of  $\Delta$ FosB. Experimental Biology, San Diego, 2014. FASEB Journal.

**Wu Q**, Mifflin SW. Time course of changes in glutamatergic transmission within the nucleus of the solitary tract during chronic intermittent hypoxia exposure and the role of  $\Delta$ FosB. Research Appreciation Day, UNT Health Science Center, 2014

**Wu Q**, Mifflin SW. Time course of changes of FosB immunoreactivity in the nucleus of the solitary tract during chronic intermittent hypoxia. Experimental Biology, Boston, 2013. FASEB Journal.

**Wu Q**, Mifflin SW. Time course of changes of FosB immunoreactivity in the nucleus of the solitary tract during chronic intermittent hypoxia. Research Appreciation Day, UNT Health Science Center, 2013

**Wu Q**, Franzke M, Cherry B, Mifflin SW.  $\Delta$ FosB in the nucleus of the solitary tract contributes to persistent increase in mean arterial pressure during exposure to chronic intermittent hypoxia. Experimental Biology, San Diego, 2012. FASEB Journal.

**Wu Q**, Franzke M, Cherry B, Mifflin SW.  $\Delta$ FosB in the nucleus of the solitary tract contributes to persistent increase in mean arterial pressure during exposure to chronic intermittent hypoxia. Research Appreciation Day, UNT Health Science Center, 2012

### **ORAL PRESENTATIONS**

**Wu Q**. The Function of  $\Delta$ FosB in the Nucleus of the Solitary Tract in Chronic Intermittent Hypoxia Induced Hypertension. Boston children's hospital-Harvard Medical School, April 2015

## **AWARDS**

American Heart Association Pre-doctoral fellowship 13PRE16970013

## TABLE OF CONTENTS

<b>TITLE</b>	<b>i</b>
<b>ACKNOWLEDGEMENTS</b>	<b>ii</b>
<b>LIST OF FIGURES</b>	<b>xiv</b>
<b>CHAPTER I</b>	<b>1</b>
<b>Introduction</b>	<b>1</b>
Obstructive sleep apnea	1
Chronic intermittent hypoxia	2
Nucleus of the solitary tract	4
FosB	5
Specific aim 1	7
Specific aim 2	7
Specific aim 3	7
Summary of Results from Specific aims	8

Significance and clinical relevance _____	9
References _____	10
<b>CHAPTER II _____</b>	<b>20</b>
<b><math>\Delta</math>FosB in NTS contributes to persistent increase in mean arterial pressure during exposure to chronic intermittent hypoxia _____</b>	<b>20</b>
<b>Abstract _____</b>	<b>21</b>
<b>Introduction _____</b>	<b>22</b>
<b>Materials and Methods _____</b>	<b>23</b>
Animals _____	23
NTS microinjections _____	23
Telemetry implantation _____	24
Chronic intermittent hypoxia protocol _____	25
Immunohistochemistry _____	25
Data Analysis and Statistics _____	27
<b>Results _____</b>	<b>27</b>
Effects of dominant negative $\Delta$ FosB construct on responses to CIH in conscious rats _____	27
Effects of dominant negative construct in NTS on $\Delta$ FosB immunoreactivity in PVN and RVLN _____	29

<b>Discussion</b>	<b>29</b>
<b>References</b>	<b>34</b>
<b>CHAPTER III</b>	<b>43</b>
<b>Transcription factor <math>\Delta</math>FosB enhances glutamatergic transmission in NTS following chronic exposures to intermittent hypoxia</b>	<b>43</b>
<b>Abstract</b>	<b>44</b>
<b>Introduction</b>	<b>45</b>
<b>Materials and Methods</b>	<b>47</b>
Animals	47
Chronic intermittent hypoxia protocol	47
Immunohistochemistry studies	48
Electrophysiological studies	50
Labeling carotid body chemoreceptor afferent inputs	50
NTS microinjection	50
Brain slice preparation	51
Electrophysiological recording	51
Data Analysis	52
<b>Results</b>	<b>53</b>

Effect of CIH on $\Delta$ FosB immunoreactivity _____	53
Recovery after CIH exposure _____	54
Effect of CIH on glutamatergic synaptic transmission _____	54
Inhibition of $\Delta$ FosB in CIH induced glutamatergic synaptic transmission _____	55
Over-expression of $\Delta$ FosB and glutamatergic synaptic transmission _____	56
<b>Discussion</b> _____	<b>57</b>
<b>References</b> _____	<b>67</b>
<b>CHAPTER IV</b> _____	<b>85</b>
<b>SUMMARY AND CONCLUSIONS</b> _____	<b>85</b>
<b>LIMITATIONS AND FUTURE STUDIES</b> _____	<b>87</b>
<b>CHAPTER V</b> _____	<b>89</b>
<b>GENERAL DISCUSSION</b> _____	<b>89</b>
<b>Clinical significance</b> _____	<b>95</b>
<b>References</b> _____	<b>97</b>
<b>APPENDIX</b> _____	<b>100</b>

## LIST OF FIGURES

### CHAPTER II

#### Figure

1. Representative digital images of AAV-GFP- $\Delta$ JunD injection targeted at the NTS \_\_\_\_\_ 38
2. Effect of dominant-negative inhibition of NTS  $\Delta$ FosB on MAP and HR \_\_\_\_\_ 39
3. Effect of dominant-negative inhibition of NTS  $\Delta$ FosB on RF and ACT \_\_\_\_\_ 40
4. Representative digital images of FosB/ $\Delta$ FosB immunoreactivity on one side in RVLM of sham and dominant-negative rats \_\_\_\_\_ 41
5. Representative digital images of FosB/ $\Delta$ FosB immunoreactivity on one side in PVN of sham and dominant-negative rats \_\_\_\_\_ 42

### CHAPTER III

#### Figure

1. Representative digital images of  $\Delta$ FosB and DBH immunostaining and co-localization in the NTS from a control rat and a 7 day CIH rat \_\_\_\_\_ 78
2. The number of  $\Delta$ FosB immunoreactive neurons and  $\Delta$ FosB+DBH immunoreactive neurons in the NTS in normoxia and different durations of CIH exposure \_\_\_\_\_ 79
3. Effect of CIH on mEPSCs \_\_\_\_\_ 80
4. Group data of the effect of CIH on mEPSCs \_\_\_\_\_ 81
5. Effect of dominant negative blockade of NTS  $\Delta$ FosB on mEPSCs \_\_\_\_\_ 82
6. Effect of dominant negative blockade of NTS  $\Delta$ FosB on tractus-evoked inputs \_\_\_\_\_ 83

7. Effect of overexpression of $\Delta$ FosB on mEPSCs	84
--	----

## CHAPTER V

### Figure

1. Overall Conclusion	96
-----------------------	----

## APPENDIX

### Figure

1. Representative digital images of NTS slice under infrared differential contrast and fluorescence	100
2. Effect of corticosterone on mEPSCs	101
3. Combined effect of CIH and corticosterone on mEPSCs	103

## CHAPTER I

### Introduction

**Obstructive sleep apnea (OSA)** is a global syndrome and the most common type of sleep apnea (16). During sleep, the patients have completely or partially collapsed upper airways, which result in repeated periods of apneas and hypopneas (16), accompanying with oxyhemoglobin desaturation, sleep fragmentation and lead to arousal (77). Apneas are cessations in breathing for more than ten seconds and hypopneas are hypoventilatory events that have a decrease in respiratory volume by 5% for more than ten seconds. OSA has severe impacts on patient's daily life; its severity can be defined by the number of apnea and hypopnea episodes per hour of sleep (apnea-hypopnea index, AHI) as determined by polysomnography (a continuous overnight recording of sleep breathing, and cardiac parameters) (77): 5-15 defined as mild, 15-30 as moderate and greater than 30 as severe cases (65). Approximately 1 in 5 adults have at least mild OSA and 1 in 15 adults have OSA of moderate or severe intensity (77). Recent publications have shown that there are about 9% middle-aged women and 24% men suffering from OSA in America, which is a heavy burden for healthcare (16). Risk factors with the potential to suffer from OSA include overweight, central body fat distribution, large neck girth, craniofacial and upper airway abnormalities, chronic nasal congestion, aging, menopause, diabetes, use of alcohol and smoking (77). OSA is associated with many cardiovascular diseases such as systemic hypertension (7), pulmonary hypertension, arrhythmias (both bradyarrhythmias and tachyarrhythmias) (24, 35, 80), coronary heart disease, myocardial infarction, congestive heart

failure and stroke as well as metabolic disorders such as obesity, insulin resistance, diabetes and hyperlipidemias, also neurocognitive abnormalities such as daytime somnolence, decreased alertness, reduced psychomotor speed and impaired executive function (6). All of these increase the probability of morbidity and mortality (10, 36, 38, 41, 76, 77). Arterial chemoreceptor activation by hypoxemia during nocturnal apnea contributes to increased sympathetic nerve activity (SNA) which induces increased arterial pressure (AP) (30, 71). The elevation of SNA and AP in OSA patients persists even during day time when they are awake. The mechanisms underlying OSA associated persistent increased AP are not completely understood. We propose neuronal adaptations resulting from hypoxemia during night time are an important driving force for diurnal AP elevation (12). Continuous positive airway pressure (CPAP) is a standard treatment for OSA patients (8, 72). CPAP reduces blood pressure and SNA in OSA patients (8, 26, 47). In addition, CPAP can reduce pulmonary arterial blood pressure (3) and cardiovascular mortality induced by cardiac arrhythmias and stroke (9, 44). CPAP treatment of OSA for 1 month increases the ejection fraction in heart failure patients (29). Besides CPAP, there are other treatments for OSA. Mandibular advancement devices (MAD) protrude the mandible to increase the volume of pharyngeal airway and increase the upper airway muscular tone to enhance airway stability (69). Uvulopalatopharyngoplasty, tracheostomy and maxillo-mandibular advancement therapy are surgical procedures for the treatment of OSA but have severe side effects. Therefore CPAP and MAD are preferentially applied before these surgical treatments (4).

**Chronic intermittent hypoxia (CIH)** is a widely used rodent model to study OSA related ailments as it mimics the nocturnal arterial hypoxemia seen in OSA (17, 19, 20). A variety of CIH protocols exist with oxygen levels from as low as 3% to as high as 10% (23, 58, 59, 74). Animals are exposed to CIH during their sleep-cycle (day), and the oxygen saturation in these

CIH conditions is correlated with values observed in patients with OSA (28, 42). In our study, adult male Sprague-Dawley rats were exposed to CIH during their nocturnal periods from 8am to 4pm (8 hours). Nitrogen flowed into CIH chambers for 3 minutes to reduce the oxygen level to 10% for about 1 minute, then switched to room air flow for 3 minutes to return the oxygen level back to 21%, lasting about 1 minute. From 4pm rats are exposed to room air for the remainder of light period (8pm) and throughout dark period (8pm-8am) (12hours light: 12 hours dark). Considering the number of hypoxic periods in one hour during CIH, our model is comparable to mild level of sleep apnea in humans (65). Our previous data showed that the mean arterial pressure (MAP) increases during exposure to 7 days CIH. This increase occurs both in the light period when rats are exposed to hypoxia and in the dark period when rats are in room air (12, 33). There is also an increase in SNA during 7 days CIH (68). We studied responses to 7 days CIH to investigate the initial mechanisms that stimulate sympathetic outflow as the underpinning mechanism of CIH induced hypertension (33). Other laboratories using longer protocols have reported similar increases in AP and no further increase in MAP occurs after 7 days for up to 35 days of CIH (17).

Intermittent hypoxia is first sensed by arterial chemoreceptors located in the carotid and aortic body. There are type I glomus cells and type II sustentacular cells composing the arterial chemoreceptors. Glomus cells are hypoxia-sensitive and release numerous neurotransmitters in response to altered O<sub>2</sub> and CO<sub>2</sub>/H<sup>+</sup> homeostasis (22), while sustentacular cells are merely structural in nature. Intermittent hypoxia activates glomus cells, leading a release of excitatory amino acid neurotransmitters into the terminals of the carotid sinus branch of the glossopharyngeal nerve (22, 40, 56). Activated arterial chemoreceptor afferents terminate in the brainstem to initiate the arterial chemoreflex, resulting in an elevation of phrenic nerve activity,

and both sympathetic and parasympathetic nerve discharge, leading to hyperventilation, high blood pressure, and paradoxical bradycardia (37). Previous studies demonstrated that CIH increased the sensitivity of arterial chemoreceptors (63) and this increase lasted for a long time (62, 63). In addition, carotid sinus nerve sectioning prior to CIH exposure abolished the elevated blood pressure induced by CIH (19, 39). The autonomic alterations observed following hypoxia are eliminated when chemoreceptors are inhibited by hyperoxia breathing (64). These phenomena emphasize the essential role of carotid chemoreceptors and afferents in CIH induced hypertension. Collectively, CIH induced changes of blood pressure are likely mediated by a combination of the sympathetic nervous system (19), and vasoconstriction factors such as angiotensin II (Ang II), vasopressin and catecholamines (5, 16, 17, 21, 34, 67). Intermittent hypoxia is accompanied with hypercapnia during apneic episodes in OSA patients (70, 71). Cessation of hypoxia and hypercapnia cause ventilation, heart rate and arterial oxygen saturation to return to baseline levels, whereas the increase in SNA persists for a while (64). Hypoxia rather than hypercapnia is the primary stimulus for developing this prolonged augmentation in sympathetic tone (14, 73, 75). In addition, Fletcher's lab found that the MAP response to CIH was no different when it was associated with hypocapnia, eucapnia or hypercapnia (18). Based on these effects of CIH to SNA and AP, CIH is a suitable rodent model to study the mechanisms behind OSA induced high blood pressure.

**Nucleus of the solitary tract (NTS)** is an integrative site in the central nervous system: rostral NTS receives gustatory afferents; dorsomedial NTS is the location of cardiovascular afferents endings; respiratory afferent endings are found ventrally and ventrolaterally; gastrointestinal afferents terminate in sub-postremal NTS although there is clear overlap across modalities (1, 2). Among these NTS regions, the caudal NTS (caudal to calamus) receives direct input from

visceral afferents of arterial chemoreceptors, baroreceptors, volume receptors and sympathetic afferents making it a principal site to induce reflex variations in sympathetic and parasympathetic discharge along with hormonal regulation. Therefore, the NTS plays a significant role in neural cardiovascular regulation and integration (60). NTS neurons have broad cellular heterogeneity. A portion of the neurons receives afferent Solitary Tract (ST) synaptic contacts, so they are second order neurons. These neurons can be either interneurons with axonal projections contained within the NTS or projection neurons that send axons out of the NTS to other CNS areas such as PVN or RVLM (1, 2, 25). Throughout the NTS, there are neurons responding to the chemoreceptor stimulation (48). Chemoreceptor afferent terminals release glutamate as the neurotransmitter to NTS neurons (49). The glutamate binds to excitatory amino acid (EAA) receptors such as N-methyl D-aspartate (NMDA) and non-NMDA subtypes on NTS neurons to increase discharge to the pre-sympathetic neurons of RVLM. There is also evidence that PVN is involved in the chemoreflex pathway (11, 31, 57), and the PVN receives projections from NTS neurons. The PVN can increase SNA by projections to the RVLM and/ or projections to the sympathetic pre-ganglionic neurons in the intermediate lateral (IML) of spinal cord (1). Activation of sympathetic pre-ganglionic neurons causes vasoconstriction (27) and a release of catecholamines from the adrenal medulla (61). CIH induces changes in the synaptic activation of NTS neurons (32) and increases responses to exogenous application of AMPA and NMDA (15).

**FosB** is a member of the Fos family of transcription factors, which dimerize with a Jun family member to form the activator protein (AP)-1 complex, which binds to AP-1 sites in gene promoters with sequences of either TGACTCA or TGACGTCA (12, 33). Fos has been widely used as an indicator of acute as well as chronic or intermittent activation in the central nervous system (CNS) (12, 33). The Fos family includes cFos, FosB,  $\Delta$ FosB, Fos-related antigen 1

(Fra1), and Fra2. Each of these has its own time course of expression in response to acute or chronic stimuli (12, 45, 46, 50, 53). Among these transcription factors, cFos expression is the fastest and transient, so it is a predominant marker for acute stimulation (13, 66). The truncated splice variant of the fos gene,  $\Delta$ FosB, has stable expression for several days, so it is an important factor in inducing and maintaining long-term plasticity in the brain associated with various conditions, such as drug addiction, epilepsy, Parkinson's disease, depression, and antidepressant treatment (43, 46, 51, 52, 54, 55, 78).  $\Delta$ FosB is also a potent marker for a wide range of chronic, intermittent stimulation such as stress and substance abuse (52). Another feature of  $\Delta$ FosB is that it has different functions over time. It acts as a transcriptional repressor at AP-1 sites with short-term treatments, but functions as a transcriptional activator when it accumulates with more chronic treatments (12, 46). Previous studies have used FosB staining as a marker for neural activation following exposure to CIH (33, 34). FosB expression has also been shown to increase in response to in vitro and in vivo exposure to intermittent hypoxia (33). Our lab has shown that the number of FosB immunoreactive neurons in NTS is significantly increased after 7 days of CIH exposure, as well as in RVLM, A5 regions of the hindbrain and organum vasculosum of the lamina terminalis (OVLT), median preoptic nucleus (MnPO), subfornical organ (SFO), and PVN regions of the forebrain. These regions are involved in endocrine control and sympathetic outflow regulation (33). The persistent elevation of MAP during exposure to CIH, together with the increase of FosB staining in autonomic and endocrine regulatory regions of CNS, provides a possible clue of the molecular basis of CIH induced hypertension. A recent publication showed that  $\Delta$ FosB in MnPO mediates transcriptional activity of downstream target genes angiotensin converting enzyme 1 (ACE 1) and ACE 2, and blocking  $\Delta$ FosB in MnPO attenuates CIH

induced sustained high blood pressure (12). This finding suggests a linkage between  $\Delta$ FosB, SNA and renin angiotensin system activation within the MnPO.

**We hypothesize that  $\Delta$ FosB in NTS contributes to neuronal plasticity, and contributes to the persistent increase of MAP after exposures to CIH.** To address this hypothesis, three specific aims were developed.

**Specific aim 1:** Determine the relationship between  $\Delta$ FosB in NTS region and CIH induced hypertension. **Our working hypothesis is that  $\Delta$ FosB contributes to the persistent increase in MAP during exposure to CIH.** We microinjected a GFP labeled, AAV-mediated  $\Delta$ FosB dominant-negative antagonist  $\Delta$ JunD into NTS region, and also injected another group of rats with AAV-GFP as sham controls. MAP, HR, RF and activity changes in both light period and dark period in the two groups were compared in room air condition and during exposure to CIH.

**Specific aim 2:** Determine the time-course of induction of  $\Delta$ FosB immunoreactivity in NTS neurons during CIH exposure. **Our working hypothesis is that within one day of CIH exposure the number of  $\Delta$ FosB immunoreactive neurons in NTS exceeds normoxic condition levels.** We measured the number of  $\Delta$ FosB immunoreactive neurons following normoxia, 1 day, 3 days, 5 days and 7 days of CIH exposure and also 1 day normoxia after 7 days hypoxia, 3 days normoxia after 7 days hypoxia and 7 days normoxia after 7 days hypoxia. Caudal and sub-postremal NTS regions were analyzed separately.

**Specific aim 3:** Determine if  $\Delta$ FosB plays a role in mediating changes in glutamatergic transmission in NTS after CIH. CIH enhances miniature excitatory postsynaptic current (mEPSC) amplitude in second order peripheral chemoreceptor NTS neurons. **Our working hypothesis is that blocking the transcriptional function of  $\Delta$ FosB in the NTS will prevent**

**CIH-induced increase in mEPSC amplitude in second order NTS neurons.** AAV mediated viral vectors were microinjected into NTS. DiA labeling of the carotid body region enabled visualization of chemoreceptor synaptic terminals on NTS neurons (15, 79). mEPSCs from neurons labeled with both GFP and DiA fluorescence were recorded in a dominant negative group, sham control group and non-CIH exposure group.

### **Summary of Results from Specific aims**

In the first specific aim,  $\Delta$ FosB blockade attenuated the CIH-induced increase of MAP in both the light and dark phases, but MAP in sham control rats was maintained. To understand the upstream and downstream pathways that might contribute to these changes,  $\Delta$ FosB immunoreactivity was examined in the PVN and RVLM. In PVN, the number of  $\Delta$ FosB immunoreactive cells was significantly reduced after functional blocking NTS  $\Delta$ FosB, while no significant change in the number of  $\Delta$ FosB immunoreactive cells was observed in RVLM after  $\Delta$ FosB blockade in NTS.

The second specific aim examined  $\Delta$ FosB immunoreactivity in NTS at different durations of CIH.  $\Delta$ FosB increased within 1 day CIH, and remained elevated throughout the 7 days of CIH. Following 1 day recovery after 7 days CIH  $\Delta$ FosB immunoreactivity had returned to normoxia level. Within 1 day CIH and throughout 7 days of CIH, MAP is significantly increased (33), consistent with our result that the expression of  $\Delta$ FosB significantly increased after 1 day of CIH and remained elevated during a 7 day exposure. This time course in the induction of  $\Delta$ FosB provides information about at what time point  $\Delta$ FosB expression increases and therefore may contribute to cardiovascular regulative function.

The third specific aim was to elucidate the role of  $\Delta$ FosB in glutamatergic transmission in NTS after CIH exposure. We found that the time course of the increase in mEPSC amplitude during different durations of CIH exposure is quite similar to changes in the time course of FosB/ $\Delta$ FosB immunoreactivity. Furthermore, NTS  $\Delta$ FosB blockade abolished the increase in amplitude of mEPSCs observed in NTS neurons from CIH rats. A viral vector overexpressing  $\Delta$ FosB in NTS increased mEPSC amplitude like CIH. These results suggest that  $\Delta$ FosB in NTS neurons might mediate molecular adaptations and plasticity which play an essential role in the sustained hypertensive response to CIH. Further studies to quantify the post-translational modifications in AMPA receptor subunits might explain the mechanism behind this elevation in amplitude of mEPSCs in arterial chemoreceptor NTS second order neurons.

### **Significance and clinical relevance**

This research is among the first to attempt to identify the transcription factors that mediate neuronal adaptation and plasticity to CIH. To date, the role of  $\Delta$ FosB in the regulation of cardiovascular responses has not been well clarified. Our study provides an understanding of the central neuronal mechanisms of CIH induced hypertension and suggests potential targets for clinical therapy.

## **References**

1. **Andresen MC, Doyle MW, Bailey TW, and Jin YH.** Differentiation of autonomic reflex control begins with cellular mechanisms at the first synapse within the nucleus tractus solitarius. *Braz J Med Biol Res* 37: 549-558, 2004.
2. **Andresen MC and Kunze DL.** Nucleus tractus solitarius--gateway to neural circulatory control. *Annu Rev Physiol* 56: 93-116, 1994.
3. **Arias MA, Garcia-Rio F, Alonso-Fernandez A, Martinez I, and Villamor J.** Pulmonary hypertension in obstructive sleep apnoea: effects of continuous positive airway pressure: a randomized, controlled cross-over study. *Eur Heart J* 27: 1106-1113, 2006.
4. **Aurora RN, Casey KR, Kristo D, Auerbach S, Bista SR, Chowdhuri S, Karippot A, Lamm C, Ramar K, Zak R, and Morgenthaler TI.** Practice parameters for the surgical modifications of the upper airway for obstructive sleep apnea in adults. *Sleep* 33: 1408-1413.
5. **Bao G, Randhawa PM, and Fletcher EC.** Acute blood pressure elevation during repetitive hypocapnic and eucapnic hypoxia in rats. *J Appl Physiol (1985)* 82: 1071-1078, 1997.
6. **Beebe DW, Groesz L, Wells C, Nichols A, and McGee K.** The neuropsychological effects of obstructive sleep apnea: a meta-analysis of norm-referenced and case-controlled data. *Sleep* 26: 298-307, 2003.
7. **Bradley TD and Floras JS.** Obstructive sleep apnoea and its cardiovascular consequences. *Lancet* 373: 82-93, 2009.
8. **Bratel T, Wennlund A, and Carlstrom K.** Pituitary reactivity, androgens and catecholamines in obstructive sleep apnoea. Effects of continuous positive airway pressure treatment (CPAP). *Respir Med* 93: 1-7, 1999.

9. **Campos-Rodriguez F, Martinez-Garcia MA, de la Cruz-Moron I, Almeida-Gonzalez C, Catalan-Serra P, and Montserrat JM.** Cardiovascular mortality in women with obstructive sleep apnea with or without continuous positive airway pressure treatment: a cohort study. *Ann Intern Med* 156: 115-122.
10. **Conde SV, Sacramento JF, Guarino MP, Gonzalez C, Obeso A, Diogo LN, Monteiro EC, and Ribeiro MJ.** Carotid body, insulin, and metabolic diseases: unraveling the links. *Front Physiol* 5: 418.
11. **Cruz JC, Bonagamba LG, Machado BH, Biancardi VC, and Stern JE.** Intermittent activation of peripheral chemoreceptors in awake rats induces Fos expression in rostral ventrolateral medulla-projecting neurons in the paraventricular nucleus of the hypothalamus. *Neuroscience* 157: 463-472, 2008.
12. **Cunningham JT, Knight WD, Mifflin SW, and Nestler EJ.** An Essential role for DeltaFosB in the median preoptic nucleus in the sustained hypertensive effects of chronic intermittent hypoxia. *Hypertension* 60: 179-187.
13. **Cunningham JT, Penny ML, and Murphy D.** Cardiovascular regulation of supraoptic neurons in the rat: synaptic inputs and cellular signals. *Prog Biophys Mol Biol* 84: 183-196, 2004.
14. **Cutler MJ, Swift NM, Keller DM, Wasmund WL, and Smith ML.** Hypoxia-mediated prolonged elevation of sympathetic nerve activity after periods of intermittent hypoxic apnea. *J Appl Physiol (1985)* 96: 754-761, 2004.
15. **de Paula PM, Tolstykh G, and Mifflin S.** Chronic intermittent hypoxia alters NMDA and AMPA-evoked currents in NTS neurons receiving carotid body chemoreceptor inputs. *Am J Physiol Regul Integr Comp Physiol* 292: R2259-2265, 2007.

16. **Dempsey JA, Veasey SC, Morgan BJ, and O'Donnell CP.** Pathophysiology of sleep apnea. *Physiol Rev* 90: 47-112.
17. **Fletcher EC, Bao G, and Li R.** Renin activity and blood pressure in response to chronic episodic hypoxia. *Hypertension* 34: 309-314, 1999.
18. **Fletcher EC, Bao G, and Miller CC, 3rd.** Effect of recurrent episodic hypocapnic, eucapnic, and hypercapnic hypoxia on systemic blood pressure. *J Appl Physiol (1985)* 78: 1516-1521, 1995.
19. **Fletcher EC, Lesske J, Behm R, Miller CC, 3rd, Stauss H, and Unger T.** Carotid chemoreceptors, systemic blood pressure, and chronic episodic hypoxia mimicking sleep apnea. *J Appl Physiol (1985)* 72: 1978-1984, 1992.
20. **Fletcher EC, Lesske J, Qian W, Miller CC, 3rd, and Unger T.** Repetitive, episodic hypoxia causes diurnal elevation of blood pressure in rats. *Hypertension* 19: 555-561, 1992.
21. **Foster GE, Hanly PJ, Ahmed SB, Beaudin AE, Pialoux V, and Poulin MJ.** Intermittent hypoxia increases arterial blood pressure in humans through a Renin-Angiotensin system-dependent mechanism. *Hypertension* 56: 369-377.
22. **Gonzalez C, Almaraz L, Obeso A, and Rigual R.** Carotid body chemoreceptors: from natural stimuli to sensory discharges. *Physiol Rev* 74: 829-898, 1994.
23. **Gozal D, Daniel JM, and Dohanich GP.** Behavioral and anatomical correlates of chronic episodic hypoxia during sleep in the rat. *J Neurosci* 21: 2442-2450, 2001.
24. **Guilleminault C, Connolly SJ, and Winkle RA.** Cardiac arrhythmia and conduction disturbances during sleep in 400 patients with sleep apnea syndrome. *Am J Cardiol* 52: 490-494, 1983.

25. **Guyenet PG.** Neural structures that mediate sympathoexcitation during hypoxia. *Respiration Physiology* 121: 147-162, 2000.
26. **Haentjens P, Van Meerhaeghe A, Moscariello A, De Weerd S, Poppe K, Dupont A, and Velkeniers B.** The impact of continuous positive airway pressure on blood pressure in patients with obstructive sleep apnea syndrome: evidence from a meta-analysis of placebo-controlled randomized trials. *Arch Intern Med* 167: 757-764, 2007.
27. **Hudson S, Johnson CD, and Marshall JM.** Changes in muscle sympathetic nerve activity and vascular responses evoked in the spinotrapezius muscle of the rat by systemic hypoxia. *J Physiol* 589: 2401-2414.
28. **Jun J, Reinke C, Bedja D, Berkowitz D, Bevans-Fonti S, Li J, Barouch LA, Gabrielson K, and Polotsky VY.** Effect of intermittent hypoxia on atherosclerosis in apolipoprotein E-deficient mice. *Atherosclerosis* 209: 381-386.
29. **Kaneko Y, Floras JS, Usui K, Plante J, Tkacova R, Kubo T, Ando S, and Bradley TD.** Cardiovascular effects of continuous positive airway pressure in patients with heart failure and obstructive sleep apnea. *N Engl J Med* 348: 1233-1241, 2003.
30. **Kara T, Narkiewicz K, and Somers VK.** Chemoreflexes--physiology and clinical implications. *Acta Physiol Scand* 177: 377-384, 2003.
31. **King TL, Heesch CM, Clark CG, Kline DD, and Hasser EM.** Hypoxia activates nucleus tractus solitarius neurons projecting to the paraventricular nucleus of the hypothalamus. *Am J Physiol Regul Integr Comp Physiol* 302: R1219-1232.
32. **Kline DD, Ramirez-Navarro A, and Kunze DL.** Adaptive depression in synaptic transmission in the nucleus of the solitary tract after in vivo chronic intermittent hypoxia: evidence for homeostatic plasticity. *J Neurosci* 27: 4663-4673, 2007.

33. **Knight WD, Little JT, Carreno FR, Toney GM, Mifflin SW, and Cunningham JT.** Chronic intermittent hypoxia increases blood pressure and expression of FosB/DeltaFosB in central autonomic regions. *Am J Physiol Regul Integr Comp Physiol* 301: R131-139.
34. **Knight WD, Saxena A, Shell B, Nedungadi TP, Mifflin SW, and Cunningham JT.** Central losartan attenuates increases in arterial pressure and expression of FosB/DeltaFosB along the autonomic axis associated with chronic intermittent hypoxia. *Am J Physiol Regul Integr Comp Physiol* 305: R1051-1058.
35. **Koehler U, Fus E, Grimm W, Pankow W, Schafer H, Stammnitz A, and Peter JH.** Heart block in patients with obstructive sleep apnoea: pathogenetic factors and effects of treatment. *Eur Respir J* 11: 434-439, 1998.
36. **Krieger J, McNicholas WT, Levy P, De Backer W, Douglas N, Marrone O, Montserrat J, Peter JH, and Rodenstein D.** Public health and medicolegal implications of sleep apnoea. *Eur Respir J* 20: 1594-1609, 2002.
37. **Kumar P.** Systemic effects resulting from carotid body stimulation-invited article. *Adv Exp Med Biol* 648: 223-233, 2009.
38. **Lee W, Nagubadi S, Kryger MH, and Mokhlesi B.** Epidemiology of Obstructive Sleep Apnea: a Population-based Perspective. *Expert Rev Respir Med* 2: 349-364, 2008.
39. **Lesske J, Fletcher EC, Bao G, and Unger T.** Hypertension caused by chronic intermittent hypoxia--influence of chemoreceptors and sympathetic nervous system. *J Hypertens* 15: 1593-1603, 1997.
40. **Lopez-Barneo J.** Oxygen and glucose sensing by carotid body glomus cells. *Curr Opin Neurobiol* 13: 493-499, 2003.

41. **Lopez-Jimenez F, Sert Kuniyoshi FH, Gami A, and Somers VK.** Obstructive sleep apnea: implications for cardiac and vascular disease. *Chest* 133: 793-804, 2008.
42. **Louis M and Punjabi NM.** Effects of acute intermittent hypoxia on glucose metabolism in awake healthy volunteers. *J Appl Physiol (1985)* 106: 1538-1544, 2009.
43. **Madsen TM, Bolwig TG, and Mikkelsen JD.** Differential regulation of c-Fos and FosB in the rat brain after amygdala kindling. *Cell Mol Neurobiol* 26: 87-100, 2006.
44. **Martinez-Garcia MA, Soler-Cataluna JJ, Ejarque-Martinez L, Soriano Y, Roman-Sanchez P, Illa FB, Canal JM, and Duran-Cantolla J.** Continuous positive airway pressure treatment reduces mortality in patients with ischemic stroke and obstructive sleep apnea: a 5-year follow-up study. *Am J Respir Crit Care Med* 180: 36-41, 2009.
45. **McClung CA and Nestler EJ.** Neuroplasticity mediated by altered gene expression. *Neuropsychopharmacology* 33: 3-17, 2008.
46. **McClung CA, Ulery PG, Perrotti LI, Zachariou V, Berton O, and Nestler EJ.** DeltaFosB: a molecular switch for long-term adaptation in the brain. *Brain Res Mol Brain Res* 132: 146-154, 2004.
47. **McNicholas WT.** Cardiovascular outcomes of CPAP therapy in obstructive sleep apnea syndrome. *Am J Physiol Regul Integr Comp Physiol* 293: R1666-1670, 2007.
48. **Mifflin SW.** Arterial chemoreceptor input to nucleus tractus solitarius. *Am J Physiol* 263: R368-375, 1992.
49. **Mizusawa A, Ogawa H, Kikuchi Y, Hida W, Kurosawa H, Okabe S, Takishima T, and Shirato K.** In vivo release of glutamate in nucleus tractus solitarii of the rat during hypoxia. *J Physiol* 478 ( Pt 1): 55-66, 1994.

50. **Nanduri J, Yuan G, Kumar GK, Semenza GL, and Prabhakar NR.** Transcriptional responses to intermittent hypoxia. *Respir Physiol Neurobiol* 164: 277-281, 2008.
51. **Nestler EJ.** Is there a common molecular pathway for addiction? *Nat Neurosci* 8: 1445-1449, 2005.
52. **Nestler EJ.** Molecular basis of long-term plasticity underlying addiction. *Nat Rev Neurosci* 2: 119-128, 2001.
53. **Nestler EJ.** Molecular mechanisms of drug addiction. *Neuropharmacology* 47 Suppl 1: 24-32, 2004.
54. **Nestler EJ.** Molecular neurobiology of addiction. *Am J Addict* 10: 201-217, 2001.
55. **Nestler EJ, Barrot M, and Self DW.** DeltaFosB: a sustained molecular switch for addiction. *Proc Natl Acad Sci U S A* 98: 11042-11046, 2001.
56. **Nurse CA.** Neurotransmitter and neuromodulatory mechanisms at peripheral arterial chemoreceptors. *Exp Physiol* 95: 657-667.
57. **Olivan MV, Bonagamba LG, and Machado BH.** Involvement of the paraventricular nucleus of the hypothalamus in the pressor response to chemoreflex activation in awake rats. *Brain Res* 895: 167-172, 2001.
58. **Peng YJ, Overholt JL, Kline D, Kumar GK, and Prabhakar NR.** Induction of sensory long-term facilitation in the carotid body by intermittent hypoxia: implications for recurrent apneas. *Proc Natl Acad Sci U S A* 100: 10073-10078, 2003.
59. **Polotsky VY, Rubin AE, Balbir A, Dean T, Smith PL, Schwartz AR, and O'Donnell CP.** Intermittent hypoxia causes REM sleep deficits and decreases EEG delta power in NREM sleep in the C57BL/6J mouse. *Sleep Med* 7: 7-16, 2006.

60. **Potts JT, Paton JF, Mitchell JH, Garry MG, Kline G, Anguelov PT, and Lee SM.** Contraction-sensitive skeletal muscle afferents inhibit arterial baroreceptor signalling in the nucleus of the solitary tract: role of intrinsic GABA interneurons. *Neuroscience* 119: 201-214, 2003.
61. **Prabhakar NR, Kumar GK, and Peng YJ.** Sympatho-adrenal activation by chronic intermittent hypoxia. *J Appl Physiol (1985)* 113: 1304-1310.
62. **Prabhakar NR, Peng YJ, Jacono FJ, Kumar GK, and Dick TE.** Cardiovascular alterations by chronic intermittent hypoxia: importance of carotid body chemoreflexes. *Clin Exp Pharmacol Physiol* 32: 447-449, 2005.
63. **Prabhakar NR, Peng YJ, Kumar GK, Nanduri J, Di Giulio C, and Lahiri S.** Long-term regulation of carotid body function: acclimatization and adaptation--invited article. *Adv Exp Med Biol* 648: 307-317, 2009.
64. **Querido JS, Kennedy PM, and Sheel AW.** Hyperoxia attenuates muscle sympathetic nerve activity following isocapnic hypoxia in humans. *J Appl Physiol (1985)* 108: 906-912.
65. **Ruehland WR, Rochford PD, O'Donoghue FJ, Pierce RJ, Singh P, and Thornton AT.** The new AASM criteria for scoring hypopneas: impact on the apnea hypopnea index. *Sleep* 32: 150-157, 2009.
66. **Rylski M and Kaczmarek L.** Ap-1 targets in the brain. *Front Biosci* 9: 8-23, 2004.
67. **Saxena A, Little JT, Nedungadi TP, and Cunningham JT.** Angiotensin II type 1a receptors in subfornical organ contribute towards chronic intermittent hypoxia-associated sustained increase in mean arterial pressure. *Am J Physiol Heart Circ Physiol* 308: H435-446.
68. **Sharpe AL, Calderon AS, Andrade MA, Cunningham JT, Mifflin SW, and Toney GM.** Chronic intermittent hypoxia increases sympathetic control of blood pressure: role of

neuronal activity in the hypothalamic paraventricular nucleus. *American Journal of Physiology-Heart and Circulatory Physiology* 305: H1772-H1780, 2013.

69. **Soll BA and George PT.** Treatment of obstructive sleep apnea with a nocturnal airway-patency appliance. *N Engl J Med* 313: 386-387, 1985.

70. **Somers VK, Mark AL, and Abboud FM.** Sympathetic activation by hypoxia and hypercapnia--implications for sleep apnea. *Clin Exp Hypertens A* 10 Suppl 1: 413-422, 1988.

71. **Somers VK, White DP, Amin R, Abraham WT, Costa F, Culebras A, Daniels S, Floras JS, Hunt CE, Olson LJ, Pickering TG, Russell R, Woo M, and Young T.** Sleep apnea and cardiovascular disease: an American Heart Association/American College of Cardiology Foundation Scientific Statement from the American Heart Association Council for High Blood Pressure Research Professional Education Committee, Council on Clinical Cardiology, Stroke Council, and Council on Cardiovascular Nursing. *J Am Coll Cardiol* 52: 686-717, 2008.

72. **Suzuki M, Otsuka K, and Guilleminault C.** Long-term nasal continuous positive airway pressure administration can normalize hypertension in obstructive sleep apnea patients. *Sleep* 16: 545-549, 1993.

73. **Tamisier R, Nieto L, Anand A, Cunningham D, and Weiss JW.** Sustained muscle sympathetic activity after hypercapnic but not hypocapnic hypoxia in normal humans. *Respir Physiol Neurobiol* 141: 145-155, 2004.

74. **Veasey SC, Zhan G, Fenik P, and Pratico D.** Long-term intermittent hypoxia: reduced excitatory hypoglossal nerve output. *Am J Respir Crit Care Med* 170: 665-672, 2004.

75. **Xie A, Skatrud JB, Puleo DS, and Morgan BJ.** Exposure to hypoxia produces long-lasting sympathetic activation in humans. *J Appl Physiol (1985)* 91: 1555-1562, 2001.

76. **Young T, Peppard PE, and Gottlieb DJ.** Epidemiology of obstructive sleep apnea: a population health perspective. *Am J Respir Crit Care Med* 165: 1217-1239, 2002.
77. **Young T, Skatrud J, and Peppard PE.** Risk factors for obstructive sleep apnea in adults. *JAMA* 291: 2013-2016, 2004.
78. **Zachariou V, Bolanos CA, Selley DE, Theobald D, Cassidy MP, Kelz MB, Shaw-Lutchman T, Berton O, Sim-Selley LJ, Dileone RJ, Kumar A, and Nestler EJ.** An essential role for DeltaFosB in the nucleus accumbens in morphine action. *Nat Neurosci* 9: 205-211, 2006.
79. **Zhang W, Carreno FR, Cunningham JT, and Mifflin SW.** Chronic sustained and intermittent hypoxia reduce function of ATP-sensitive potassium channels in nucleus of the solitary tract. *Am J Physiol Regul Integr Comp Physiol* 295: R1555-1562, 2008.
80. **Zwillich C, Devlin T, White D, Douglas N, Weil J, and Martin R.** Bradycardia during sleep apnea. Characteristics and mechanism. *J Clin Invest* 69: 1286-1292, 1982.

## **CHAPTER II**

### **$\Delta$ FosB in NTS contributes to persistent increase in mean arterial pressure during exposure to chronic intermittent hypoxia**

Running Title: FosB in NTS and CIH hypertension

Qiong Wu, Tom Cunningham and Steve W. Mifflin

Department of Integrative Physiology and Anatomy

Cardiovascular Research Institute

University of North Texas Health Science Center

Fort Worth, Texas – 76107

**To be submitted to Am J Physiol**

## **Abstract**

$\Delta$ FosB is a member of the AP-1 family of transcription factors.  $\Delta$ FosB has low constitutive expression in the central nervous system and is induced following exposure of rodents to chronic intermittent hypoxia (CIH), a model of the arterial hypoxemia that accompanies sleep apnea. We hypothesize  $\Delta$ FosB in the nucleus of solitary tract (NTS) contributes to increased mean arterial pressure (MAP) during CIH. The NTS of 11 male Sprague Dawley rats was injected (3 sites, 100nl per site) with a dominant-negative functional antagonist of  $\Delta$ FosB (adeno-associated virus (AAV)-green fluorescent protein (GFP) reporter-  $\Delta$ JunD). The NTS of 10 rats was injected with AAV-GFP as sham controls. Two weeks after NTS injections rats were exposed to CIH for 7 days, 8h/day and MAP recorded using telemetry. In the sham group 7 days CIH increased MAP from  $99.8 \pm 1.1$  mmHg to  $107.3 \pm 0.5$  mmHg in the day and from  $104.4 \pm 1.1$  mmHg to  $109.8 \pm 0.6$  in the night. In the group receiving  $\Delta$ JunD, CIH increased MAP during the day from  $95.9 \pm 1.7$  mmHg to  $101.3 \pm 0.4$  mmHg; during the dark MAP increased from  $100.9 \pm 1.7$  mmHg to  $102.8 \pm 0.5$  mmHg (both time periods compared to sham  $p < 0.05$ ). Following injection of the dominant-negative construct in the NTS, CIH-induced  $\Delta$ FosB immunoreactivity was decreased in paraventricular nucleus ( $p < 0.001$ ), however no change was observed in rostral ventro-lateral medulla. These data indicate that  $\Delta$ FosB within the NTS contributes to the increase in MAP induced by CIH exposure.

Key words:  $\Delta$ FosB, Nucleus of the solitary tract, chronic intermittent hypoxia.

## **Introduction**

Obstructive sleep apnea (OSA) is defined as complete or partial collapse of the upper airway during sleep, leading to repeated periods of respiratory airflow ceases resulting in apnea and hypopnea (4). OSA is associated with cardiovascular and metabolic diseases (27, 29) including systemic hypertension (12, 16). Hypoxemia activates arterial chemoreceptors and chemoreceptor afferents release the excitatory amino acid neurotransmitter glutamate at synapses with NTS neurons to activate regions like paraventricular nucleus of the hypothalamus (PVN) (22, 26) and rostral ventrolateral medulla (RVLM) (9) to increase sympathetic nervous discharge (SND) and mean arterial pressure (MAP). To study OSA-induced pathologies, many labs utilize a rodent model of chronic intermittent hypoxia (CIH) which mimics the repetitive arterial hypoxemia seen in patients with sleep disordered breathing including OSA (5, 6). Like OSA patients, rats exposed to CIH show elevated arterial pressure, SND as well as both basal activity and hypoxic sensitivity of the arterial chemoreflex which contribute to systemic hypertension (5-8, 28). CIH elevates MAP and SND not only during day time when rats are exposed to intermittent hypoxia, but also throughout the normoxic night time (1, 2, 11, 14, 28).

Central mechanisms that might contribute to this persistent increase of SND and hypertension induced by CIH are currently unclear. Transcription factor FosB or its more stable splice variant  $\Delta$ FosB has been widely used as an indicator of chronic or intermittent activation in the CNS in response to drug addiction (18-21).  $\Delta$ FosB immunoreactivity is also increased in major cardiovascular regulatory regions of the CNS following exposure to CIH (1, 14, 15).

The functional role of  $\Delta$ FosB induced by exposures to CIH has been studied using AAV expressing  $\Delta$ JunD which is a dominant negative construct which functionally antagonizes  $\Delta$ FosB.

$\Delta$ JunD binds to  $\Delta$ FosB and prevents the complex from binding to AP-1 sites on DNA which inhibits the transcriptional function of  $\Delta$ FosB. Using this dominant-negative construct, Cunningham et al. demonstrated that  $\Delta$ FosB in the median preoptic nucleus (MnPO) plays a role in the sustained hypertension resulting from CIH (2). Since CIH increases the number of FosB immunoreactive neurons in the NTS (14), experiments using the same construct were performed to examine the role of  $\Delta$ FosB in the NTS on CIH-induced hypertension. To examine if CIH-induced  $\Delta$ FosB in the NTS impacts the activity of neurons downstream from NTS,  $\Delta$ FosB immunoreactivity in PVN and RVLM were also examined.

Overall, the goal of these studies was to test the hypothesis that functional antagonism of  $\Delta$ FosB function in NTS neurons during CIH will attenuate the elevated blood pressure observed during exposure to CIH and this is associated with a reduction in the transcriptional activation of neurons in PVN and RVLM.

## **Materials and methods**

**Animals.** Adult male Sprague-Dawley rats (200-250 g) from Charles River Laboratories (Wilmington, MA) were individually housed in a thermostatically regulated room with a 12 hour light: 12 hour dark cycle (on at 7 AM, off at 7 PM) and supplied with food and water ad libitum. All the experiments were performed in accordance with the NIH guidelines and with the approval of Institutional Animal Care and Use Committee of the University of North Texas Health Science Center at Fort Worth.

**NTS microinjections.** Under aseptic conditions, rats were kept on a heating pad placed in a stereotaxic frame with the head flexed to 45°, and ventilated using a nosecone with supplemental

room air and isoflurane (2%) for inhalation anesthetization. The elimination of withdrawal to a hind paw pinch was a sign of adequate anesthesia. Limited occipital craniotomy was performed to expose the hind brain at the level of calamus scriptorius. Injections of 100 nL were made at 3 sites 0.5 mm below the surface of the brain using a glass micropipette (tip diameter, 50  $\mu$ m) connected to pneumatic picopump (PV 800, WPI, Sarasota, FL) over a 5 minute period. Either an adenovirus expressing GFP and  $\Delta$ JunD (AAV-GFP- $\Delta$ JunD) or an adenovirus expressing GFP only (AAV-GFP) was injected at following coordinates: midline, 0.5 mm caudal to calamus; 0.5 mm rostral to calamus, 0.5 mm bilaterally to midline. The titer of the vectors averaged  $2.0 \times 10^7$  infectious units/ml. The dominant negative construct  $\Delta$ JunD cannot distinguish  $\Delta$ FosB from FosB, but  $\Delta$ FosB is the predominant form with the longest half-life (17-21, 30) so for the sake of simplicity we refer to  $\Delta$ FosB alone throughout this manuscript. All viral constructs were kindly provided by Dr. Eric J. Nestler (Mount Sinai Medical Center, New York). A minimum of 14 days were allowed to elapse between the NTS injection and initial baseline measurements. The presence of GFP fluorescence identifies neurons that were successfully transfected and where GFP was expressed. AAV-GFP injections were used as sham control. Post-surgery rats were placed in cages warmed by a radiant light and monitored while recovering from anesthesia. Rimadyl (0.5 mg) was provided for post-operative analgesia.

Telemetry implantation. Under isoflurane (2%) inhalation anesthesia, rats were implanted with an abdominal aortic catheter attached to a TA11PA-C40 radio-telemetry transmitter. The transmitter was secured to the abdominal muscle by aseptic surgery and was maintained in the abdominal cavity during entire post-surgical recovery, normoxia and CIH condition. The Dataquest A.R.T 2.2 telemetry system (Data Sciences International, St. Paul, MN) monitored MAP, HR, RF and activity as previously described (1, 11, 14, 15). One week is required for

recovery from surgery. Baseline data collection from the telemetry probe is acquired starting 7 days before the CIH exposure, followed by 7 days CIH data collection. Arterial pressure (AP) measurements obtained during a 10-second sampling period (500 Hz) were averaged and recorded in 10 minute intervals. Pulse interval and fluctuations obtained from the AP waveform were used to calculate HR and RF respectively. MAP, HR, and RF were averaged for every hour in the 24-h period and the 1-h averages averaged during the light phase (period of exposure) during CIH (8 AM to 4 PM) and during the dark period (7 PM to 7 AM).

Chronic Intermittent Hypoxia Protocol. Rats were individually housed in cages for a week after arrival. Following NTS microinjection surgery and recovery as well as telemetry surgery and recovery rats were relocated into custom-built plexiglass chambers that connect to the CIH system. The CIH system has been previously described (2, 14, 15). Briefly, fractional inspired O<sub>2</sub> (FIO<sub>2</sub>) was reduced from 21% to 10% in 105 s, and held at 10% for 75 s, then returned to 21% in 105 s, and held at 21% for 75 s. Each complete cycle lasted 6 minutes. Rats were exposed to CIH during the light period (8 am to 4 pm), so they were exposed to 80 CIH cycles per day. Chambers were maintained at room air (21% O<sub>2</sub>) throughout the remainder of the light period (4 h) and the dark period (12 h). Control animals were housed in identical cages in the same room and were exposed to the same ambient noise and lighting conditions as rats exposed to CIH.

Immunohistochemistry. Rats were anesthetized with thiobutabarbital (100 mg/kg i.p. Inactin; Sigma, St. Louis, MO, cat # MFCD00214068) and were transcardially perfused with 0.1 M phosphate buffered saline (PBS) followed by 300–500 ml of 4% paraformaldehyde (PFA) in PBS in the morning after the last CIH exposure. Brains were post fixed in PFA at room temperature for 1-2 h and then transferred into 30% sucrose at 4°C for dehydration until submerged. Each brain stem was embedded in cryostat compound (Tissue TEK OCT, Sakura

Finetek USA, Inc., Torrance, CA) and three sets of coronal 40  $\mu$ m sections were collected by using a cryostat microtome (Leica CM1950, Leica Microsystems Inc., Buffalo Grove, IL). All the sections were stored in cryoprotectant at -20°C until processed for immunohistochemistry. Brain stem sections were incubated in goat polyclonal anti-FosB (Santa Cruz Biotechnology, Santa Cruz, CA; 1:5000, sc-48) at 4°C for 48 h. The anti-FosB antibody does not discriminate full length FosB from the splice variant  $\Delta$ FosB. Sections were then processed with biotinylated horse anti-goat IgG (Vector Laboratories, Burlingame, CA; 1:100, BA-9500) and reacted with an avidin-peroxidase conjugate (Vectastain ABC Kit; Vector Laboratories, Burlingame, CA, PK-4000 ) for 1 h and then treated with PBS containing 0.04% nickel ammonium sulfate and 0.04% 3,3'-diaminobenzidine hydrochloride for 11 minutes. The FosB-stained brain stem sections were processed with mouse anti-TH primary antibody (1:1,000, MAB318; Millipore) and a CY3-labeled donkey anti-mouse secondary antibody (1:1200, 715-165-150; Jackson Immuno-Research). Forebrain sections were processed FosB/ $\Delta$ FosB staining as described above. Sections were mounted on gelatin-coated slides and air dried for 2 days and then coverslipped with Permount. Sections were visualized under an Olympus microscope (BX41) equipped for epifluorescence and an Olympus DP70 digital camera with DP manager software (v 2.2.1). Images were uniformly adjusted for brightness and contrast. The rat brain stereotaxic atlas of Paxinos and Watson (23) was used to for identify specific regions. All counts were performed using ImageJ software (v 1.44, National Institutes of Health, Bethesda, MD). Sections double labeled for TH-FosB were used to count FosB/ $\Delta$ FosB immunoreactivity in RVLM and 9 to 10 sections were analyzed for NTS and RVLM; 5 to 6 sections for PVN [2 to 3 sections per rat/subnuclei dorsal parvocellular (dp), medial parvocellular (mp), lateral parvocellular (lp), and posterior magnocellular (pm)] were analyzed from each rat. The number of immunoreactive

neurons per section was averaged for each rat and these were then averaged to obtain the group mean.

Data Analysis and Statistics. Two-way repeated-measures analysis of variance (ANOVA) and Student-Neuman-Keuls (SNK) post-hoc analysis were used to compare the difference between baseline and daily measurements of MAP, HR, RF and activity over the 7 days of CIH. Light phase and dark phase were analyzed separately. FosB/ $\Delta$ FosB immunoreactivity counts in PVN and RVLM across different groups were compared by one-way ANOVA with the SNK test for post hoc analysis.  $P < 0.05$  was considered significant.

## **Results**

### *Effects of dominant negative $\Delta$ FosB construct on responses to CIH in conscious rats.*

Histological examination of the injection sites showed that AAV construct produced intense GFP labeling in the NTS. (Fig. 1) Figure 2, 3 illustrate the averaged MAP, HR, RF and activity in the light period (left) and the dark period (right) in conscious rats during CIH. Seven days of control baseline values were recorded in both groups of rats. There was no significant difference between the baselines of these parameters comparing AAV-GFP and AAV-GFP- $\Delta$ JunD groups during the light or dark phases.

There was an interaction for MAP during the light phase (treatment  $\times$  day interaction,  $P < 0.05$ ). Follow-up analysis of the interaction indicated that MAP during the light phase was significantly higher on all days of CIH compared to baseline in both AAV-GFP and AAV-GFP- $\Delta$ JunD groups (Fig. 2A;  $P < 0.001$ ). There was also an interaction for MAP during the dark phase (treatment  $\times$  day interaction,  $P < 0.05$ ). MAP in the AAV-GFP group was significantly higher

compared to baseline on all days of CIH ( $P < 0.001$ ) with the exception of CIH day 1, but was only significantly elevated on CIH day 4 ( $P < 0.05$ ) in AAV-GFP- $\Delta$ JunD group. The AAV-GFP- $\Delta$ JunD- treated rats showed a significantly reduced CIH-induced increase in MAP compared with AAV-GFP-treated rats during the dark phase (Fig. 2B;  $P < 0.001$ ). In the light phase, AAV-GFP- $\Delta$ JunD- treated rats also showed an attenuation of the elevated MAP compared with AAV-GFP-treated rats (Fig. 2A;  $P < 0.05$ ).

During the light phase, HR was significantly influenced by the treatments (treatment  $\times$  day interaction,  $P < 0.05$ ). In CIH day 1, 2, 3, 4 there was no significant difference from baseline level while in CIH day 5, 6, 7, HR significantly decreased compared to baseline in AAV-GFP group (Fig. 2C;  $P < 0.05$ ). In AAV-GFP- $\Delta$ JunD group, CIH day 1 and day 2 significantly increased HR compared to baseline (Fig. 2C;  $P < 0.05$ ), but no change of HR in other CIH days. In the dark period, HR were not significantly influenced by the treatments (treatment  $\times$  day interaction,  $P > 0.05$ ). There was no significant difference in HR between two groups in either light phase or dark phase (Fig. 2C, D).

Both in the light phase and dark phase, there were not significant interactions for RF (treatment  $\times$  day interaction,  $P > 0.05$ ). There was no significant difference in RF between two groups in either light phase or dark phase (Fig. 3A, B).

Activity (ACT) in the light period was significantly influenced by interactions (treatment  $\times$  day interaction,  $P < 0.05$ ). ACT significantly decreased in all CIH days compared with baseline in the light phase in AAV-GFP rats (Fig. 3C;  $P < 0.001$ ), but significantly increased in AAV-GFP- $\Delta$ JunD rats (Fig. 3C;  $P < 0.05$ ). In the dark phase, no significant influence of interactions exist

(treatment  $\times$  day interaction,  $P > 0.05$ ). There was no significant difference between AAV-GFP and AAV-GFP- $\Delta$ JunD groups in either the light or dark phase (Fig. 3C, D).

*Effects of dominant negative construct in NTS on  $\Delta$ FosB immunoreactivity in RVLM and PVN.*

To further determine the effects of dominant negative inhibition of NTS  $\Delta$ FosB on the chronic transcriptional activation of autonomic regulatory regions of the CNS during CIH,  $\Delta$ FosB immunoreactivity was examined in RVLM and PVN. There was no difference of CIH-induced  $\Delta$ FosB immunoreactivity in RVLM after injection of the dominant-negative construct into NTS (Fig. 4C). While the  $\Delta$ FosB staining in RVLM was intermingled with TH-positive neurons, there was no significant co-localization of  $\Delta$ FosB with TH (sham:  $0.1 \pm 0.04$ ; dominant negative:  $0.4 \pm 0.1$ ). Injection of dominant-negative construct in NTS significantly decreased CIH-induced  $\Delta$ FosB immunoreactivity in PVN compared to the sham group (sham:  $21.0 \pm 4.7$ ; dominant negative:  $10.8 \pm 1.8$ ,  $n=7$ ). Analysis of PVN subregions revealed significant reductions in dorsal parvocellular, medial parvocellular, lateral parvocellular and posterior magnocellular subnuclei (Fig. 5C;  $P < 0.05$ ).

## **Discussion**

The results of the present study provide the first evidence that  $\Delta$ FosB in the NTS plays an important role in CIH-induced hypertension. Functional antagonism of FosB in the NTS reduced CIH-induced increased MAP during both the day time, when exposed to intermittent hypoxia, and during the night time when normoxic. AAV-GFP- $\Delta$ JunD rats attenuated the increase of MAP while AAV-GFP rats still maintained an elevation of MAP compared to normoxic controls. These results imply that  $\Delta$ FosB within NTS mediates the hypertensive response to CIH.

CIH and OSA alter both the peripheral (24, 25) and central (3, 13, 25, 31) components of the arterial chemoreflex and leads to increased sympathetic nerve activity and hypertension. A 7 day exposure to CIH increases arterial pressure (1, 2, 11, 14, 15, 28), during both the day time and the night time and also increases  $\Delta$ FosB immunoreactivity in CNS autonomic and endocrine regulatory regions such as NTS, PVN, and RVLM (14) suggesting a causal link between  $\Delta$ FosB expression and CIH hypertension. After inhibition of  $\Delta$ FosB function in NTS by the dominant-negative construct, CIH-induced hypertension was reduced in both the light period when rats were exposed to CIH, and during the night time when rats were exposed to room air. Therefore,  $\Delta$ FosB in NTS plays a role in CIH-induced hypertension.

To further investigate potential sites in the CNS downstream from NTS that might be involved in the reduction in MAP during CIH following blockade of  $\Delta$ FosB in NTS,  $\Delta$ FosB immunoreactivity was examined in sympatho-regulatory sites such as PVN and RVLM. Inhibition of NTS  $\Delta$ FosB reduced  $\Delta$ FosB immunoreactivity in PVN but not in RVLM. This suggests that  $\Delta$ FosB in PVN induced by CIH is dependent upon  $\Delta$ FosB in NTS, whereas  $\Delta$ FosB in RVLM is not. The lack of change in RVLM is surprising as it is known glutamatergic inputs from NTS to RVLM play an important role in chemoreflex sympathoexcitation (10). However, our dominant-negative injections did not totally abolish  $\Delta$ FosB in NTS and perhaps the remaining neurons were sufficient to drive  $\Delta$ FosB in RVLM, but not in PVN. It is also important to remember that  $\Delta$ FosB is but one of any number of transcription factors that can mediate neuronal plasticity. Functional blockade of  $\Delta$ FosB in MnPO reduced CIH hypertension and  $\Delta$ FosB immunoreactivity in PVN and RVLM (2), so perhaps  $\Delta$ FosB in RVLM is driven by PVN inputs. Alternatively,  $\Delta$ FosB in RVLM may be generated in response to tissue hypoxia during CIH. Consistent with our previous studies, we found little evidence of co-localization of  $\Delta$ FosB

and TH within the RVLM (1, 14). Perhaps non-TH RVLM neurons exhibiting  $\Delta$ FosB after CIH might be involved in other aspects of the response to CIH, e.g. respiration, upper airway patency, etc. There is possibility that PVN sympatho-excitatory neurons might have a greater contribution to the dark phase elevation of blood pressure from baseline, while the RVLM might be more involved in the light phase hypoxia exposure.

In conclusion,  $\Delta$ FosB in NTS contributes to the CIH-induced hypertension, although the underlying mechanisms where by FosB might alter NTS neuronal function have not been described.

### **Acknowledgments**

The authors gratefully acknowledge the financial support of NIH (HL PO1-088052) and American Heart Association Pre-Doctoral Fellowship (13PRE16970013). The authors gratefully acknowledge Dr. Eric Nestler, Mount Sinai School of Medicine, for providing the dominant-negative and overexpression viral constructs.

## **Figure legends**

Figure 1. Representative digital images of AAV-GFP- $\Delta$ JunD injection targeted at the NTS. GFP labeling neurons were illustrated. cc = central canal. Scale bar: 100  $\mu$ m

Figure 2. Effect of dominant-negative inhibition of NTS  $\Delta$ FosB on MAP and HR. In each graph on x-axis, normoxic baseline values are averaged and represented as control; 7 days of CIH are represented as ih1 to ih7. A: CIH caused a significant elevation in MAP starting from day 1 in both AAV-GFP (sham) and AAV-GFP- $\Delta$ JunD (dominant-negative) injected groups, compared with their baseline, during light phase ( $P < 0.001$ ). Compared two groups, dominant-negative injection attenuated this elevation in MAP ( $P < 0.05$ ). B. during dark phase, dominant-negative injection reduced CIH induced elevation in MAP to baseline level, while sham group maintained the sustained high level of MAP. Compared two groups, dominant-negative group significantly reduced sustained component of high blood pressure occurred in sham group ( $P < 0.001$ ). C, D. HR in sham and dominant-negative groups during light phase (C) and dark phase (D). No significant difference between two groups in both phases.

Figure 3. Effect of dominant-negative inhibition of NTS  $\Delta$ FosB on RF and ACT. A, B. RF in sham and dominant-negative groups during light phase (A) and dark phase (B). No significant difference between sham and dominant negative groups in both phases. C, D. ACT in sham and dominant-negative groups during light phase (C) and dark phase (D). No significant difference between two groups in both phases.

Figure 4. Representative digital images of FosB/ $\Delta$ FosB immunoreactivity on one side in RVLM of sham (A) and dominant-negative (B) rats. C. mean no. of FosB/ $\Delta$ FosB-positive cells counted in the RVLM. n=7 in each group.

Figure 5. Representative digital images of FosB/ $\Delta$ FosB immunoreactivity on one side in PVN of sham (A) and dominant-negative (B) rats. C. mean no. of FosB/ $\Delta$ FosB-positive cells counted in the PVN. n=7 in each group.

## Reference

1. **Bathina CS, Rajulapati A, Franzke M, Yamamoto K, Cunningham JT, and Mifflin S.** Knockdown of tyrosine hydroxylase in the nucleus of the solitary tract reduces elevated blood pressure during chronic intermittent hypoxia. *Am J Physiol Regul Integr Comp Physiol* 305: R1031–R1039, 2013.
2. **Cunningham JT, Knight WD, Mifflin SW, and Nestler EJ.** An Essential role for DeltaFosB in the median preoptic nucleus in the sustained hypertensive effects of chronic intermittent hypoxia. *Hypertension* 60: 179-187.
3. **de Paula PM, Tolstykh G, and Mifflin SW.** Chronic intermittent hypoxia alters NMDA and AMPA-evoked currents in NTS neurons receiving carotid body chemoreceptor inputs. *Am J Physiol* Articles In Press: doi:10.1152/ajpregu.00760.02006, 2007.
4. **Dempsey JA, Veasey SC, Morgan BJ, and O'Donnell CP.** Pathophysiology of sleep apnea. *Physiol Rev* 90: 47-112, 2010.
5. **Fletcher EC.** Sympathetic over activity in the etiology of hypertension of obstructive sleep apnea. *Sleep* 26: 15-19, 2003.
6. **Fletcher EC, Lesske J, Behm R, Miller CC, 3rd, Stauss H, and Unger T.** Carotid chemoreceptors, systemic blood pressure, and chronic episodic hypoxia mimicking sleep apnea. *J Appl Physiol* 72: 1978-1984, 1992.
7. **Fletcher EC, Lesske J, Qian W, Miller CC, and Unger T.** Repetitive, episodic hypoxia causes diurnal elevation of blood pressure in rats. *Hypertension* 19: 555-561, 1992.
8. **Greenberg HE, Sica A, Batson D, and Scharf SM.** Chronic intermittent hypoxia increases sympathetic responsiveness to hypoxia and hypercapnia. *J Appl Physiol* 86: 298-305, 1999.

9. **Guyenet PG.** Neural structures that mediate sympathoexcitation during hypoxia. *Respiration Physiology* 121: 147-162, 2000.
10. **Guyenet PG.** The sympathetic control of blood pressure. *Nat Rev Neurosci* 7: 335-346, 2006.
11. **Hinojosa-Laborde C and Mifflin SW.** Sex differences in blood pressure response to intermittent hypoxia in rats. *Hypertension* 46: 1016-1021, 2005.
12. **Kapa S, Kuniyoshi FHS, and Somers V.** Sleep apnea and hypertension: Interactions and implications for management. *Hypertension* 51: 605-608, 2008.
13. **Kline D, Ramirez-Navarro A, and Kunze DL.** Adaptive depression in synaptic transmission in the nucleus of the solitary tract after in vivo chronic intermittent hypoxia: Evidence for homeostatic plasticity. *J Neurosci* 27: 4663-4673, 2007.
14. **Knight WD, Little JT, Carreno FR, Toney GM, Mifflin SW, and Cunningham JT.** Chronic intermittent hypoxia increases blood pressure and expression of FosB/delta FosB in central autonomic regions. *Am J Physiol Regul Integr Comp Physiol* 301: R131–R139, 2011.
15. **Knight WD, Saxena A, Shell B, Nedungadi TP, Mifflin SW, and Cunningham JT.** Central losartan attenuates increases in arterial pressure and expression of FosB/ $\Delta$ FosB along the autonomic axis associated with chronic intermittent hypoxia. *Am J Physiol Regul Integr Comp Physiol* 305: R1051-R1058, 2013.
16. **Konecny T, Kara T, and Somers V.** Obstructive sleep apnea and hypertension: An update. *Hypertension* 63: 203-209, 2014.
17. **McClung CA, Ulery PG, Perrotti L, Zachariou V, Berton O, and Nestler EJ.** DeltaFosB: a molecular switch for long-term adaptation in the brain. *Mol Br Res* 132: 146-154, 2004.

18. **Nestler EJ.** Is there a common molecular pathway for addiction? *Nat Neurosci* 8: 1145-1149, 2005.
19. **Nestler EJ.** Molecular basis of long-term plasticity underlying addiction. *Nat Rev Neurosci* 2: 119-128, 2001.
20. **Nestler EJ.** Molecular neurobiology of addiction. *Am J Addiction* 10: 201-217, 2001.
21. **Nestler EJ, Barrot M, and Self DW.** DeltaFosB: a sustained molecular switch for addiction. *Proc Natl Acad Sci* 98: 11042-11046, 2001.
22. **Olivan MV, Bonagamba LG, and Machado BH.** Involvement of the paraventricular nucleus of the hypothalamus in the pressor response to chemoreflex activation in awake rats. *Brain Research* 895: 167-172, 2001.
23. **Paxinos G and Watson C.** The Rat Brain in Stereotaxic Coordinates. *Third ed San Diego: Academic Press*, 1997.
24. **Peng Y, Kline DD, Dick TE, and Prabhakar NR.** Chronic intermittent hypoxia enhances carotid body chemoreceptor response to low oxygen. *Advances in Experimental Medicine & Biology* 499: 33-38, 2001.
25. **Ramirez J-M, Garcia III AJ, Anderson TM, Koschnitzky JE, Peng Y-J, Kumar GK, and Prabhakar NR.** Central and peripheral factors contributing to obstructive sleep apneas. *Resp Physiol and Neurobiol* 189: 344-353, 2013.
26. **Reddy MK, Patel KP, and Schultz HD.** Differential role of the paraventricular nucleus of the hypothalamus in modulating the sympathoexcitatory component of peripheral and central chemoreflexes. *Am J Physiol* 289: R789-R797, 2005.
27. **Shamsuzzaman AS, Gersh BJ, and Somers V.** Obstructive sleep apnea: Implications for cardiac and vascular disease. *J Amer Med Assoc* 290: 1906-1914, 2003.

28. **Sharpe AL, Calderon AS, Andrade MA, Cunningham JT, Mifflin SW, and Toney GM.** Chronic intermittent hypoxia increases sympathetic control of blood pressure: role of neuronal activity in the hypothalamic paraventricular nucleus. *Am J Physiol Heart Circ Physiol* 305: H1772–H1780, 2013.
29. **Xie W, Zheng F, and Song X.** Obstructive sleep apnea and serious adverse outcomes in patients with cardiovascular or cerebrovascular disease: A PRISMA-compliant systematic review and meta-analysis. *Medicine* 93: 1-8, 2014.
30. **Zachariou V, Bolanos CA, Selley DE, Theobald D, Cassidy MP, Kelz MB, Shaw-Lutchman T, Berton O, Sim-Selley LJ, Dileone RJ, Kumar A, and Nestler EJ.** An essential role for DeltaFosB in the nucleus accumbens in morphine action. *Nat Neurosci* 9: 205-211, 2006.
31. **Zhang W, Carreno FR, Cunningham JT, and Mifflin SW.** Chronic sustained and intermittent hypoxia reduce function of ATP-sensitive potassium channels in nucleus of the solitary tract. *Am J Physiol* 295: doi:10.1152/ajpregu.90390.92008, 2008.

AAV-GFP- $\Delta$ JunD injection

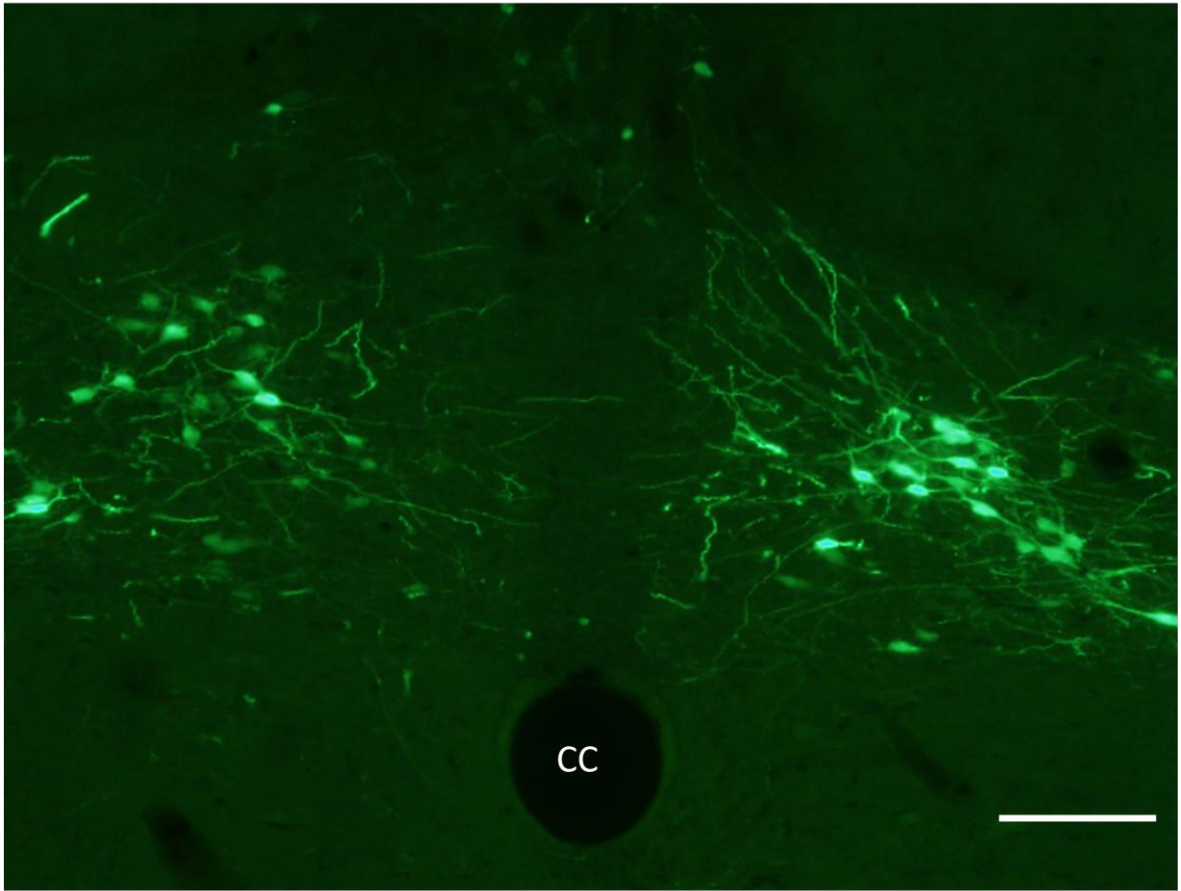


Figure 1

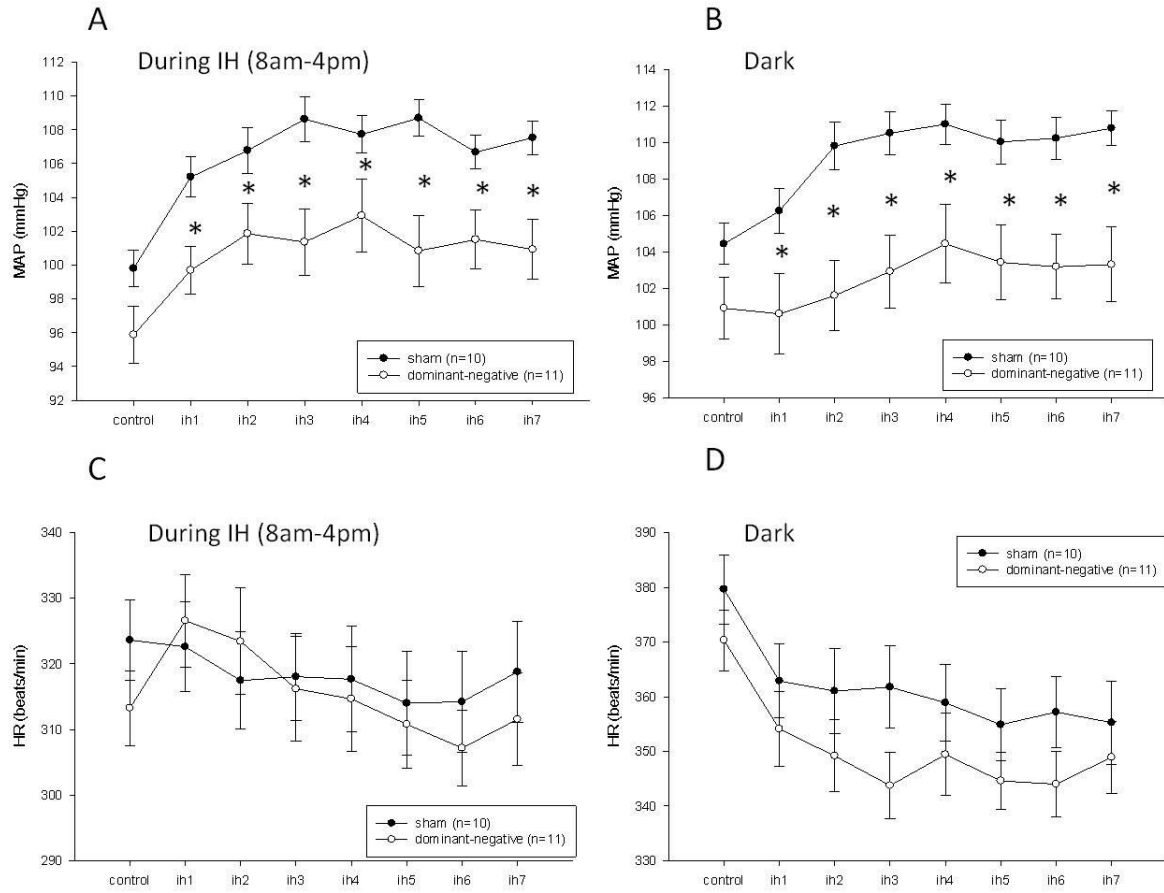


Figure 2

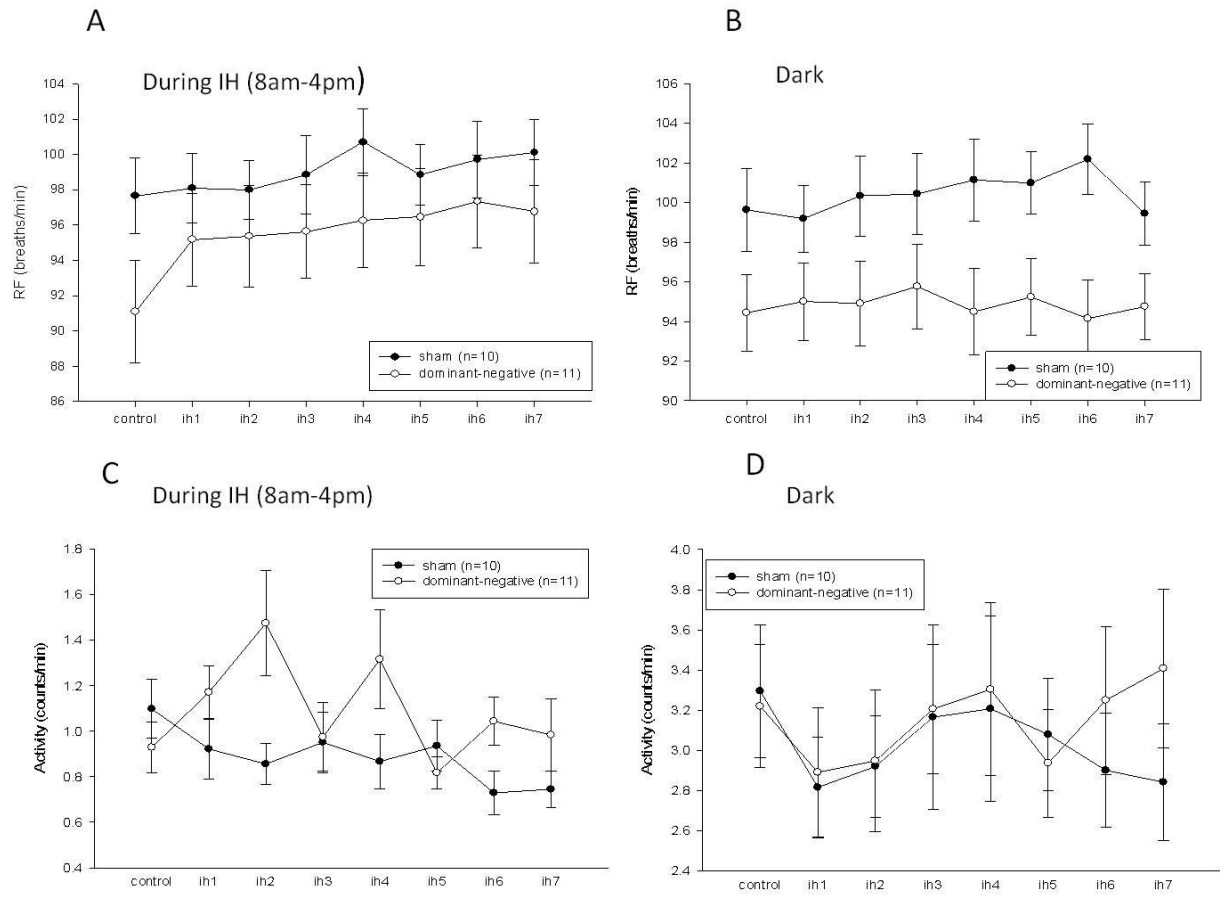
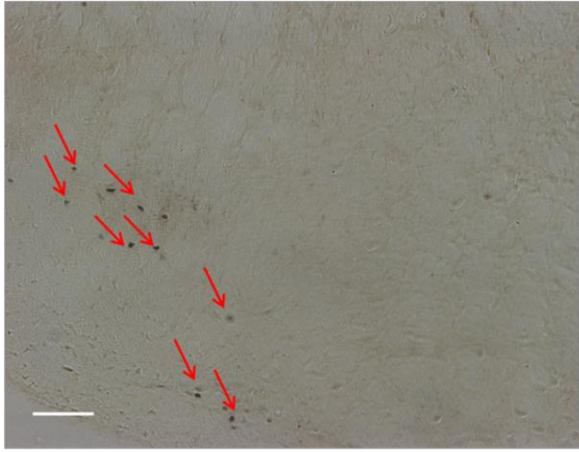


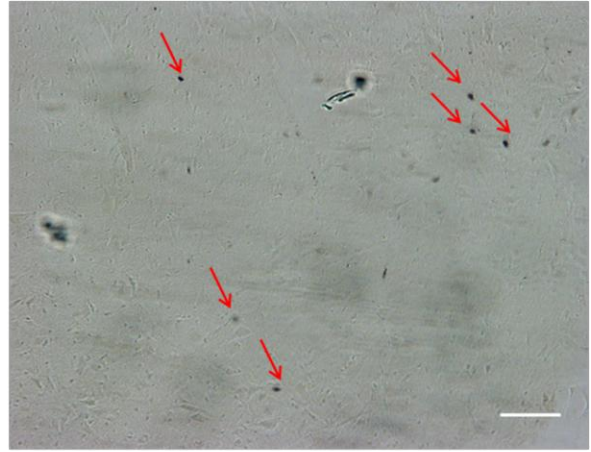
Figure 3

A



Sham virus injection

B



Dominant-negative virus injection

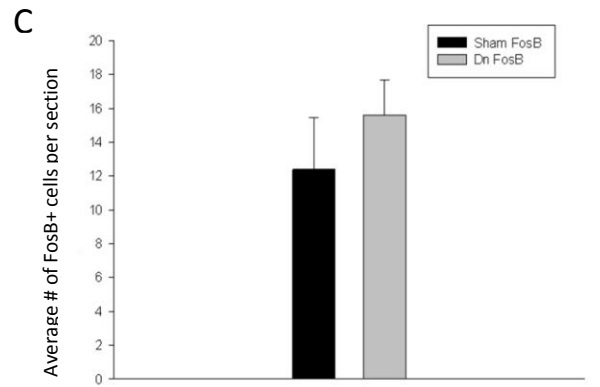
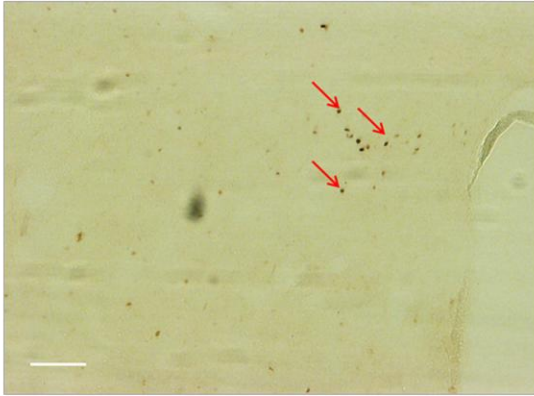


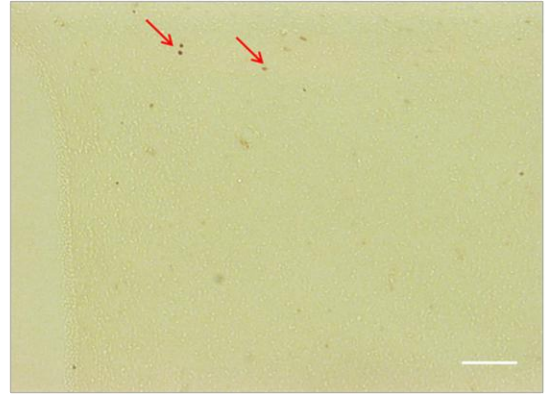
Figure 4

A



Sham virus injection

B



Dominant-negative virus injection

C

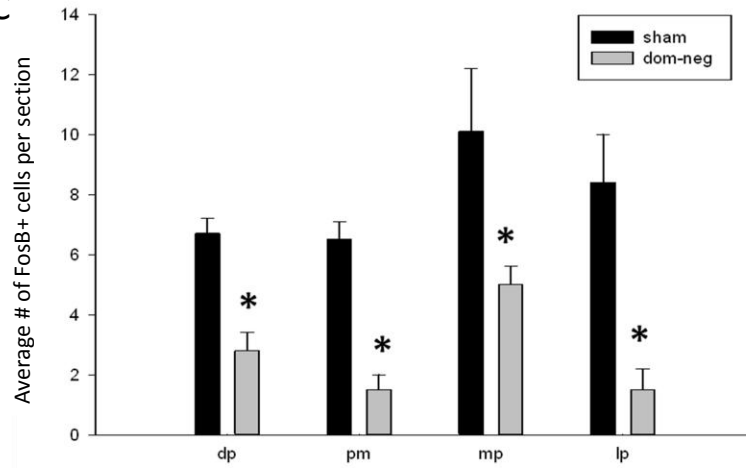


Figure 5

## **CHAPTER III**

# **Transcription factor $\Delta$ FosB enhances glutamatergic transmission in NTS following chronic exposures to intermittent hypoxia**

Running Title:  $\Delta$ FosB mediates CIH-induced changes in NTS neurons

Qiong Wu and Steve W. Mifflin

Department of Integrative Physiology and Anatomy

and Cardiovascular Research Institute

University of North Texas Health Science Center

Fort Worth, Texas – 76107

**Submitted to Am J Physiol Regul Integr Comp Physiol**

## **Abstract**

We have reported that mean arterial pressure (MAP) and the number of  $\Delta$ FosB immunoreactive neurons in the nucleus of solitary tract (NTS) are increased after 7 days of exposure to chronic intermittent hypoxia (CIH; alternating 3 min periods of increasing hypoxia to an end-point of 10% O<sub>2</sub> with 3 min 21% O<sub>2</sub> from 8 am-4 pm). To determine the time course of  $\Delta$ FosB expression and effect, male Sprague Dawley rats were exposed to either room air (control) or to CIH for 1, 3, 5 or 7 days.  $\Delta$ FosB immunoreactivity significantly increased between 1 to 7 days of CIH exposure compared to controls ( $p < 0.05$ ). Whole cell patch clamp recordings in second order arterial chemoreceptor NTS neurons in an in vitro brain slice revealed that miniature excitatory post-synaptic current (mEPSC) amplitude increased between 1 and 7 days of CIH ( $p < 0.05$  vs. normoxia), while 7 days of CIH reduced the amplitude of tractus evoked EPSCs (eEPSCs). After 1 day recovery following a 7 day exposure, mEPSC amplitude remained increased; after 3 days recovery mEPSC amplitude was similar to control, normoxic levels. A dominant-negative construct, adeno-associated virus-green fluorescent protein (GFP)- $\Delta$ JunD, was injected into NTS to block transcriptional effects of  $\Delta$ FosB. After 1 and 7 days of CIH exposure, GFP labeled second order NTS neurons had mEPSC and eEPSC amplitudes no different than control. CIH induces  $\Delta$ FosB which rapidly enhances the post-synaptic response of NTS receiving arterial chemoreceptor inputs to glutamatergic synaptic inputs which provides a potential mechanism for CIH induced hypertension.

Key words:  $\Delta$ FosB, Nucleus of the solitary tract; chronic intermittent hypoxia.

## **Introduction**

Obstructive sleep apnea (OSA), the most common type of sleep apnea, occurs when patients have completely or partially collapsed upper airways during sleep which leads to repeated periods of apneas and hypopneas (13). OSA is associated with cardiovascular and metabolic disease (61, 70). Significantly, systemic hypertension is often associated with OSA (26, 31). An important mechanism of OSA associated hypertension is an elevation of sympathetic nerve discharge (SND) (39-41, 64). A causal relationship exists between the OSA-induced hypoxemias and increased mean arterial pressure (MAP) and SND as treatment with continuous positive airway pressure during sleep eliminates the apneas and reduces MAP and SND (5, 32, 37, 60).

Chronic intermittent hypoxia (CIH) mimics the repetitive arterial hypoxemia seen in patients with OSA (17, 18). Like OSA patients, rats exposed to CIH exhibit increased MAP, SND and both basal activity and hypoxic sensitivity of the arterial chemoreflex which contribute to systemic hypertension (16-18, 20). A 7 day exposure to CIH increases MAP and SND during the day when the rats are exposed to the intermittent hypoxia and the elevated MAP persists during the night when the rats are normoxic (4, 9, 23, 29, 30, 62). This indicates that CIH induces mechanisms that sustain increased MAP and SND into the non-hypoxic periods of the diurnal cycle.

Arterial chemoreceptor afferent fibers increase their discharge during systemic hypoxia and the afferent terminals release glutamate within the nucleus of the solitary tract (NTS), a brainstem visceral integrative site of the central nervous system (CNS). Glutamate binds to excitatory amino acid (EAA) receptors e.g. N-methyl D-aspartate (NMDA) and non-NMDA subtypes on second order caudal NTS neurons (68, 76, 77) leading to enhanced discharge which is relayed to

sympatho-excitatory sites such as the paraventricular nucleus (PVN) (48, 57) and rostral ventrolateral medulla (RVLM) (4, 22) to increase SND.

The neuronal mechanisms which mediate the sustained increase in SND and hypertension following exposure to CIH are currently unknown. Transcription factor FosB and its more stable splice variant  $\Delta$ FosB are widely used as indicators of chronic, intermittent activation in the CNS (4, 29, 30, 46).  $\Delta$ FosB is a member of the Fos family of transcription factors, which dimerize with Jun family to form the activator protein (AP)-1 complex, which binds to AP-1 sites in gene promoters with the sequence either TGACTCA or TGACGTCA (42, 43, 46). Nestler et al. utilized an adeno associated virus expressing  $\Delta$ JunD.  $\Delta$ JunD binds to  $\Delta$ FosB to keep the complex from binding to AP-1 sites on DNA which inhibits  $\Delta$ FosB function. Using this dominant negative construct of  $\Delta$ FosB Nestler's group has demonstrated that  $\Delta$ FosB in the CNS mediates neuroplasticity that contributes to drug addiction (42-44, 46).

Seven days of CIH exposure significantly increased the number of neurons expressing  $\Delta$ FosB in regions involved in endocrine control and sympathetic outflow regulation (NTS, RVLM, A5, organum vasculosum of the lamina terminalis, median preoptic nucleus, subfornical organ, and PVN) (29). Increased  $\Delta$ FosB in autonomic and endocrine regulatory regions of CNS suggests that this transcription factor might contribute to changes in neurons that mediate CIH induced sustained increase in MAP and SND. Cunningham et al. demonstrated that blockade of  $\Delta$ FosB function in the median preoptic nucleus reduces CIH induced hypertension (9).

Exposure to CIH has been shown to alter NTS neuronal responses to exogenous and synaptically released glutamate. de Paula et al. demonstrated that 7 days of CIH enhanced the amplitude of AMPA-evoked currents and decreased the amplitude of NMDA-evoked currents in NTS neurons

receiving carotid body chemoreceptor inputs (12). Kline et al. showed that 10 days of CIH increased NTS neuronal discharge initiated by spontaneous transmitter release but decreased the amplitude of solitary tract-evoked excitatory post-synaptic currents (EPSCs) (28). A subsequent study reported a reduced number of excitatory synapses in NTS after CIH (2) which could explain the reduced tractus-evoked EPSC after CIH. Whether  $\Delta$ FosB in NTS neurons plays a role in the CIH induced alterations in post-synaptic responses to glutamate has not been examined. The goals of these studies were to define the time-course of  $\Delta$ FosB expression during and after CIH and to determine the effects of blocking  $\Delta$ FosB function in the NTS during exposure to CIH on spontaneous and evoked glutamatergic synaptic transmission.

## **Materials and methods**

*Animals:* Adult male Sprague-Dawley rats (200-250 g) from Charles River Laboratories (Wilmington, MA) were housed individually in a thermostatically regulated room with a 12 hour light: 12 hour dark cycle (on at 7 AM, off at 7 PM) and supplied with food and water ad libitum. All experiments were performed in accordance with the NIH guidelines and with the approval of Institutional Animal Care and Use Committee of the University of North Texas Health Science Center at Fort Worth.

*Chronic Intermittent Hypoxia Protocol:* Rats were individually housed in cages for a week after arrival, and then relocated into custom-built plexiglass chambers that connect to the CIH system. The CIH system has been previously described (23, 29, 30). Briefly, fractional inspired O<sub>2</sub> (FIO<sub>2</sub>) was reduced from 21% to 10% in 105 s, FIO<sub>2</sub> was held at 10% for 75 s then returned to 21% in 105 s, and held at 21% for 75 s. Each complete cycle lasted 6 minutes. Rats were

exposed to CIH during the light period (8 AM to 4 PM). Chambers were maintained at room air (21% O<sub>2</sub>) throughout the remainder of the light period (4 h) and the dark period (12 h). Control animals were housed in identical cages in the same room and were exposed to the same ambient noise and lighting conditions as rats exposed to CIH.

*Immunohistochemistry studies:* Rats were separated into eight groups: normoxia, 1 day CIH, 3 days CIH, 5 days CIH, 7 days CIH, (n=7 for each CIH group and 14 for the normoxia group) as well as 7 days CIH+ 1 day normoxic recovery (n=6), 7 days CIH+ 3 days normoxic recovery (n=5), 7 day CIH+ 7 days normoxic recovery (n=2). In the morning of the day after the last CIH exposure, rats were anesthetized with thiobutabarbital (100 mg/kg i.p. Inactin; Sigma, St. Louis, MO, cat # MFCD00214068) and transcardially perfused with 0.1 M phosphate buffered saline (PBS) followed by 300–500 ml of 4% paraformaldehyde (PFA) in PBS. Brains were post fixed in PFA at room temperature for 1-2 h and then transferred into 30% sucrose at 4°C until submerged. Each brain stem was embedded in cryostat compound (Tissue TEK OCT, Sakura Finetek USA, Inc., Torrance, CA) and three sets of coronal 40 µm sections were collected by using a cryostat microtome (Leica CM1950, Leica Microsystems Inc., Buffalo Grove, IL). All the sections were stored in cryoprotectant at -20°C until processed for immunohistochemistry. Sections were incubated in goat polyclonal anti-FosB/ΔFosB (Santa Cruz Biotechnology, Santa Cruz, CA; 1:5000, cat # sc-48) at 4°C for 48 h. The primary antibody used in this study does not discriminate between ΔFosB and full-length FosB; here we referred to it as ΔFosB immunoreactivity due to its being the only species that is expressed outside of acute stimulation conditions (36, 42-47, 65, 73). Sections were then processed with biotinylated mouse anti-goat IgG (Vector Laboratories, Burlingame, CA; 1:100, cat # z0326) and reacted with an avidin-peroxidase conjugate (Vectastain ABC Kit; Vector Laboratories, Burlingame, CA, cat # PK-

4000 ) for 1 h and then treated with PBS containing 0.04% nickel ammonium sulfate and 0.04% 3,3'-diaminobenzidine hydrochloride for 11 minutes. Sections were then processed for dopamine-beta-hydroxylase (DBH) staining using a mouse anti-DBH primary antibody (Millipore, Billerica, MA; 1:1000, cat # MAB394), incubated at 4°C for 48 h. DBH is a marker of catecholaminergic neurons. Sections were then incubated in a CY3-labeled donkey anti-mouse secondary antibody (Jackson ImmunoResearch, West Grove, PA; 1:1200, cat # 715-165-140) at room temperature for 4-5 h. Sections were mounted on gelatin-coated slides and air dried for 2 days and then coverslipped with Permount. Sections were visualized under a confocal microscope (Olympus IX50, Tokyo) equipped with a disk spin unit (IX2-DSU, Olympus), a motorized stage and a mercury lamp epifluorescence system. Images were captured using a Retiga-SRV camera (Q-imaging, Surrey, British Columbia, Canada) and collected using HCSImage software (Hamamatsu Corp, Bridgewater, NJ). Images were uniformly adjusted for brightness and contrast. The rat brain stereotaxic atlas of Paxinos and Watson (49) was used to identify specific regions. Images of  $\Delta$ FosB staining were collected using bright field filter. Images of DBH staining were obtained using CY3 filter.  $\Delta$ FosB counting and DBH counting were performed by ImageJ software (v 1.44, NIH, Bethesda, MD). Eight to twelve sections were analyzed from each rat NTS between 1mm rostral and 1mm caudal to the calamus. Counts from each section were averaged and are reported as an average number of neurons per slide. To analyze double labeled sections, each  $\Delta$ FosB image was inverted, pseudo-colored and merged with the image of DBH staining in the same section. Cells with green nuclei and red cytoplasm were counted as double labeled due to the fact that  $\Delta$ FosB staining (green) is restricted to the nucleus and DBH staining (red) is cytoplasmic.

*Electrophysiological studies:* Rats were separated into nine groups: normoxic group, 1 day CIH, 3 days CIH, 5 days CIH, 7 days CIH, 7 days CIH+ 1 day normoxic recovery, 7 days CIH+ 3 days normoxic recovery, NTS injection of  $\Delta$ FosB dominant-negative construct+ 1 day CIH, NTS injection of  $\Delta$ FosB dominant-negative construct + 7 days CIH groups. All surgical procedures were performed under aseptic conditions.

Labeling carotid body chemoreceptor afferent inputs: The chemoreceptor synaptic terminals in the NTS and neurons receiving these synaptic inputs were visualized by unilaterally applied with crystals of anterograde fluorescent dye DiA (1, 1'-dilinoleyl-3, 3', 3', 3'-tetramethylindocarbocyanine, 4-chlorobenzenesulphonate) (Molecular Probes, Eugene, OR) to the carotid body region of rats anesthetized with ketamine (75 mg/kg, i.p. Fort Dodge Animal Health, Overland Park, KS) and medetomidine (0.5 mg/kg, i.p.; Pfizer Animal Health, Exton, PA) as described by our lab (12, 74, 75) and others (3, 28, 38). Anesthesia was terminated by atipamezole (1 mg/kg, i.p.; Pfizer). Postoperative analgesic Rimadyl (0.5 mg) was provided.

NTS microinjection: During surgeries, rats were kept on a heating pad placed in a stereotaxic frame with the head flexed to 45°, and ventilated using a nosecone with supplemental room air and isoflurane (2%). Adequacy of anesthesia was determined by the lack of withdrawal to a hind paw pinch. Occipital craniotomy was performed to expose the hind brain at the level of the calamus scriptorius. Injections of 100 nL were made at 3 sites 0.5 mm below the surface of the brain using a glass micropipette (tip diameter, 50  $\mu$ m) connected to pneumatic picopump (PV 800, WPI, Sarasota, FL) over a 5 minute period. Either an adenovirus expressing GFP and  $\Delta$ JunD (AAV-GFP- $\Delta$ JunD) or an adenovirus expressing GFP only (AAV-GFP) was injected at the following coordinates: midline, 0.5 mm caudal to calamus; 0.5 mm rostral to calamus, 0.5 mm bilaterally to midline. The titer of the vectors averaged  $2.0 \times 10^7$  infectious units/ml. The

dominant negative construct  $\Delta$ JunD cannot distinguish  $\Delta$ FosB from FosB, but  $\Delta$ FosB is the predominant form with the longest half-life (36, 42-47, 65, 73) so for the sake of simplicity we refer to  $\Delta$ FosB alone throughout this manuscript. In a separate group of rats, a viral construct designed to increase cellular levels of  $\Delta$ FosB was injected into the NTS. All viral constructs were kindly provided by Dr. Eric J. Nestler (Mount Sinai Medical Center, New York). A minimum of 2 weeks was allowed to elapse between the NTS injection and initial baseline measurements. The presence of GFP fluorescence identifies neurons that were successfully transfected. AAV-GFP injections were used as sham control. Post-surgery the rats were placed in cages warmed by a radiant light and monitored while recovering from anesthesia. Rimadyl (0.5 mg) was provided for post-operative analgesia.

Brain slice preparation: Rats were anesthetized by isoflurane inhalation, and the brainstem was rapidly removed and placed in ice-cold, high-sucrose, artificial cerebrospinal fluid (aCSF) continuously aerated with 95% O<sub>2</sub>+ 5% CO<sub>2</sub> and composed of (in mM): 3 KCl, 1 MgCl<sub>2</sub>, 1 CaCl<sub>2</sub>, 2 MgSO<sub>4</sub>, 1.25 NaH<sub>2</sub>PO<sub>4</sub>, 26 NaHCO<sub>3</sub>, 10 glucose, and 206 sucrose, pH=7.4. The brain stem was mounted in a vibrating microtome (VT1000S, Leica Microsystems, Bannockburn, IL) to collect coronal slices (350 $\mu$ m thickness) using a sapphire knife. Slices were incubated for 1 h in normal aCSF that was continuously aerated with 95% O<sub>2</sub>+5% CO<sub>2</sub> and contained (in mM):124 NaCl, 3 KCl, 2 MgSO<sub>4</sub>, 1.25 NaH<sub>2</sub>PO<sub>4</sub>, 26 NaHCO<sub>3</sub>, 10 glucose and 2 CaCl<sub>2</sub>, pH=7.4.

Electrophysiological recording: Whole cell voltage patch clamping was performed in the recording chamber on an upright epifluorescent microscope (Olympus BX51WI, Tokyo) equipped with infrared differential interference contrast (IR-DIC) and different optical filter sets for visualization of DiA and GFP. A single slice was held in recording chamber with a nylon mesh, submerged in normal aCSF saturated with 95% O<sub>2</sub>+ 5% CO<sub>2</sub>, with a perfusion rate of 2–3

ml/min. Patch pipettes were pulled on a pipette puller (model P-2000, Sutter Instrument, Novato, CA) from borosilicate glass capillaries with a 0.90 mm inner diameter, 1.2 mm outer diameter (WPI, Sarasota, FL). Pipettes were filled with a solution containing (in mM): 145 K-gluconate, 1 MgCl<sub>2</sub>, 10 HEPES, 1.1 EGTA, 2 Mg<sub>2</sub>ATP, and 0.3 Na<sub>3</sub>GTP, pH 7.3. Pipette resistance varied between 3 to 6 MΩ. After the patch electrode was sealed onto either a DiA labeled cell or a cell labeled with both DiA and GFP and input resistance > 1 GΩ, the membrane patch under the electrode was ruptured by suction. The cell was kept at a holding potential of -60 mV.

Recordings of postsynaptic currents began 5 min after the whole cell access was established. All images were captured with a charge-coupled device (CCD) camera (QICAM IR FAST;QIMAGING, Surrey, BC, Canada) displayed on a PC monitor with the use of QCapture software(QIMAGING, Surrey, BC, Canada). Recordings were made with an AxoPatch 200B patch-clamp amplifier and pClamp software version 10.2 (Molecular Devices, Sunnyvale, CA). The tractus was stimulated at 0.5 Hz using a bipolar electrode and recordings of tractus-evoked EPSCs (eEPSCs) were made in the presence of the GABA<sub>A</sub> receptor antagonist gabazine (25 μM, Tocris, Ballwin, MO). Recordings of spontaneous, miniature EPSCs (mEPSCs) were made in the presence of gabazine and the sodium channel blocker tetrodotoxin (TTX; 0.5 μM, Tocris, Ballwin, MO).

*Data Analysis:* In the immunohistochemistry studies a one-way analysis of variance (ANOVA) with Student Newman-Keuls (SNK) or Dunn's post-hoc analysis was used to compare the difference in number of cells between the control group and individual CIH groups. The average of 7-10 responses to tractus stimulation was used to analyze the amplitude of eEPSCs. Miniature EPSC events were detected and analyzed with MiniAnalysis software (Synaptosoft Inc., v6.0, Fort Lee, NJ) 5 min duration of recordings with more than 200 events were analyzed and were

visually checked to ensure measurements were made of physiological signals. mEPSCs were detected as events that exceeded a threshold of 5 times the RMS baseline noise and frequency was calculated as the reciprocal of the interval between these events. Values are presented as mean  $\pm$  SEM. One-way ANOVA and SNK post-hoc analysis were used to compare the difference in amplitude and frequency of mEPSCs and the amplitude of eEPSCs among the normoxia group, different CIH exposure groups and NTS injection groups for electrophysiological studies. Values of  $p \leq 0.05$  were considered significant.

## **Results**

*Effect of CIH on  $\Delta$ FosB immunoreactivity:* Figure 1 illustrates the general pattern of  $\Delta$ FosB (A&B) and DBH (C&D) immunoreactivity observed in caudal NTS in a control animal (A, C, E) and an animal exposed to CIH for 7 days (B, D, F). In agreement with our previous studies (4, 29) exposure to CIH increased the number of  $\Delta$ FosB immunoreactive neurons throughout the NTS. After a 7 day exposure to CIH a small number of the  $\Delta$ FosB immunoreactive neurons also exhibited immunoreactivity for DBH (Fig. 1 E, F), indicating a catecholaminergic phenotype.

The number of  $\Delta$ FosB immunoreactive neurons in the NTS was significantly increased after 1 day of CIH and remained significantly elevated compared to control throughout the 7 day exposure ( $p < 0.01$ ) (Fig. 2A).

The number of NTS neurons exhibiting immunoreactivity for both  $\Delta$ FosB and DBH was not significantly different from control rats after 1, 3 and 5 days of CIH (Fig. 2B). However, 7 days of CIH exposure significantly increased the number of  $\Delta$ FosB and DBH immunoreactive neurons compared to control and 1, 3 and 5 days of CIH ( $p < 0.05$ ). Exposure to CIH did not alter

the total number of DBH immunoreactive neurons in the regions of NTS examined. The number of DBH immunoreactive neurons averaged between  $24 \pm 4$  –  $44 \pm 4$  neurons for control, 1-7 days of CIH and 1-7 days recovery from CIH.

Recovery after CIH exposure: To evaluate the duration of the effect of CIH on  $\Delta$ FosB expression, rats were returned to normoxic conditions for either 1, 3 or 7 days after a 7 day exposure to CIH. The number of NTS neurons exhibiting  $\Delta$ FosB immunoreactivity, with or without DBH immunoreactivity, was significantly less on all recovery days compared to 7 days CIH ( $p < 0.05$ ) (Fig. 2A&B). There was no significant difference between the number of  $\Delta$ FosB immunoreactive NTS neurons, with or without DBH immunoreactivity, on any recovery day compared to control.

Effect of CIH on glutamatergic synaptic transmission: An in vitro brain slice preparation was used to study mEPSCs and eEPSCs in NTS neurons receiving arterial chemoreceptor inputs. mEPSCs represent action potential-independent spontaneous glutamate release from pre-synaptic terminals. All data were obtained from second-order neurons in the NTS, identified by the presence of DiA labeling (Fig. 3A, B). Slices were superfused with a bath solution containing gabazine (25  $\mu$ M) to block GABA<sub>A</sub> receptors and the sodium channel blocker TTX (0.5  $\mu$ M). The mEPSCs were mediated by AMPA glutamate receptor as they were completely abolished by the non-NMDA receptor antagonist CNQX (10  $\mu$ M) (data not shown). Cumulative probabilities of the amplitude and inter event interval under no CIH and during 1 day of CIH in the same neuron as illustrated in A and B were compared. CIH neuron recording shifted rightward in the amplitude whereas no change of inter event interval between no CIH and CIH groups (Fig. 3D). The amplitude and frequency of mEPSCs in second order arterial chemoreceptor NTS neurons in control rats were compared to rats exposed to CIH for 1, 3, 5, and 7 days. Within 1 day of

exposure to CIH, mEPSC amplitude was significantly increased and remained elevated after 3, 5 and 7 days CIH exposure (Fig. 4A). mEPSCs amplitudes remained increased after 1 day of normoxic recovery and were not different compared to control amplitudes after 3 days of recovery. There was no significant difference in the frequency of mEPSCs comparing control ( $1.0 \pm 0.1$  Hz, n=12) to 1 ( $1.0 \pm 0.2$  Hz, n=11), 3 ( $1.3 \pm 0.3$  Hz, n=11), 5 ( $0.9 \pm 0.1$  Hz, n=21) and 7 days ( $0.8 \pm 0.1$  Hz, n=7) exposure to CIH. There was no difference between these values and those recorded after 1 day recovery ( $0.9 \pm 0.2$  Hz, n=4) or 3 days recovery ( $1.0 \pm 0.2$  Hz, n=7) (Fig. 4B).

*Inhibition of  $\Delta$ FosB in CIH induced glutamatergic synaptic transmission:* Two weeks after microinjection of the dominant negative viral construct (AAV-GFP- $\Delta$ JunD), we recorded mEPSCs from NTS neurons with GFP and DiA labeling after 1 and 7 days exposure to CIH (Fig. 5). In these experiments we used 2 control groups to ensure that the NTS microinjection of the viral construct did not induce a non-specific change in glutamatergic transmission; one control group received no NTS injection (CIH 1 and 7 Day, Fig. 5C) and the other control group received an NTS injection of the viral construct lacking the ability to bind  $\Delta$ FosB (AAV-GFP) (CIH 1 and 7 Day sham, Fig. 5C).

Exposure to 1 and 7 days of CIH significantly increased mEPSC amplitude in both control groups compared to rats not exposed to CIH (Fig. 5C). In rats injected with dominant negative construct, after 1 and 7 days of CIH mEPSC amplitudes were significantly less than both control, CIH-exposed groups. In rats injected with dominant negative construct, mEPSC amplitudes in CIH-exposed rats were no different than those measured in rats not exposed to CIH. The frequencies of mEPSCs were not different between any of the groups: normoxic, non-CIH exposed rats ( $1.0 \pm 0.1$  Hz, n=12); 1 day CIH no NTS injection ( $1.0 \pm 0.1$  Hz, n=11); 7 days CIH

no NTS injection ( $1.0 \pm 0.1$  Hz,  $n=19$ ); 1 day CIH sham virus injection ( $1.5 \pm 0.1$  Hz,  $n=13$ ); 7 day CIH sham virus injection ( $0.9 \pm 0.1$  Hz,  $n=18$ ). There was no difference in mEPSC amplitude or frequency comparing the control group that received no NTS injection to the other control group that received an NTS injection of the viral construct lacking the ability to bind  $\Delta$ FosB (AAV-GFP), indicating the NTS injection, the AAV nor expression of GFP altered mEPSC properties.

In contrast to the spontaneous release of glutamate, indicated by mEPSCs, CIH produces a reduction in tractus eEPSCs (28). We found a similar reduction in eEPSC amplitude after 7 days of CIH ( $p < 0.05$ ; Fig. 6). We utilized the dominant-negative  $\Delta$ JunD construct to determine if  $\Delta$ FosB plays a role in this attenuation. Examination of GFP-labeled neurons after 7 days of CIH revealed that the amplitude of tractus eEPSCs was not different comparing eEPSCs from sham-injected rats to rats injected with the dominant-negative  $\Delta$ JunD construct and the CIH group was significantly smaller than both the sham-injected and dn groups group (both  $p < 0.05$ ) (Fig. 6B).

*Over-expression of  $\Delta$ FosB and glutamatergic synaptic transmission:* A viral construct designed to overexpress  $\Delta$ FosB (AAV-GFP- $\Delta$ FosB) was injected into NTS and after at least 14 days of normoxic exposure, we recorded mEPSCs from NTS neurons with GFP and DiA labeling. For comparison, we also recorded from non-GFP labeled neurons which exhibited DiA labeling (Fig. 7A). The mEPSC amplitudes in the over-expression group ( $18.9 \pm 1.2$  pA,  $n=10$ ) were significantly greater than those measured in control rats ( $12.3 \pm 0.8$  pA,  $n=12$ ) ( $p < 0.001$ ; Fig. 7B). The mEPSC amplitudes in the over-expression group were not different compared to rats exposed to 7 days of CIH. There were no significant differences in the mEPSC frequency between any of the groups: normoxic control ( $1.0 \pm 0.1$  Hz,  $n=12$ ); 7 day CIH exposure ( $1.0 \pm 0.1$  Hz,  $n=12$ ); over-expression vector injection ( $0.9 \pm 0.1$  Hz,  $n=10$ ). Recordings from non-GFP

labeled neurons with DiA labeling revealed mEPSC amplitudes ( $14.5 \pm 0.4$  pA, n=13) and frequencies ( $0.8 \pm 0.1$  Hz) which were not different from the normoxic control levels.

## **Discussion**

CIH is a model of the arterial hypoxemia that occurs during OSA and has been widely used to study sleep apnea induced hypertension (4, 17, 18, 21, 23, 29, 78). CIH models expose rodents to cyclic reductions in atmospheric oxygen levels during the nocturnal period. Such exposures increase arterial pressure and SND and both remain elevated during non-hypoxic periods of the day. This indicates that CIH alters cardiovascular function to sustain chronically elevated SND and blood pressure as observed in OSA patients (6, 13, 25, 26, 31, 39-41).

We have previously reported that a 7 day exposure to CIH increases both blood pressure and the number of neurons in central cardiorespiratory regulatory regions expressing the transcription factor  $\Delta$ FosB (29). We were interested in determining the time course of increased  $\Delta$ FosB levels after exposure to CIH and if  $\Delta$ FosB might mediate alterations in glutamatergic transmission within NTS after CIH. We report that within one day of exposure to CIH, NTS neurons receiving arterial chemoreceptor afferent inputs exhibit an enhanced response to spontaneously released glutamate and that this effect of CIH is mediated by transcription factor  $\Delta$ FosB.

*CIH and glutamatergic transmission* CIH has been shown to alter both the peripheral (54-56) and central (12, 28, 56, 75) components of the arterial chemoreflex. Carotid body sensitivity is enhanced during CIH and CIH evokes a long term increase in carotid body sensitivity to hypoxia (50, 51, 53). Altered glutamatergic transmission has been demonstrated in the NTS and other CNS sites following exposure to CIH (8, 12, 28, 58, 63, 66). Our lab has previously

demonstrated that CIH increased inward current induced by exogenous application of AMPA (12). Enhanced afferent inputs to the CNS from arterial chemoreceptors coupled with increased neuronal excitation in response to glutamatergic chemoreceptor afferent inputs following exposures to CIH provides a substrate for persistently enhanced chemoreflex activation and sustained elevation of blood pressure and SND upon return to normoxia. While mechanisms that could mediate the enhanced responses of the chemoreceptors after CIH have been described (52), there is less information on the mechanisms that mediate central facilitation of the chemoreflex.

Kline et al. reported that tractus evoked EPSCs (EPSCs) were depressed after 10 days of CIH exposure (28) and our observations are consistent with this finding. Kline et al suggested that this depression was evidence for homeostatic synaptic plasticity (67) in an attempt to normalize NTS neuronal discharge which is increased during exposure to CIH due to increased arterial chemoreceptor afferent induced excitation. CIH induced depression of tractus eEPSCs could be mediated by a reduction of the number of active synapses reported to occur after 10 days of CIH (2). The reduced eEPSC is not consistent with a model of CIH hypertension driven by increased NTS discharge in response to chemoreceptor afferent inputs. However, in vitro stimulation of the tractus synchronously activates afferent inputs at low frequency. In vivo, asynchronous afferent volleys occur at much higher frequencies so temporal summation could overcome the spatial factors that reduce eEPSC amplitude. It is important to remember that rodents (20, 24, 33) and humans (1, 10, 11, 34) exposed to IH as well as sleep apnea patients (19, 25, 41) exhibit enhanced chemoreflex responses to acute hypoxia and arterial chemoreceptor “drive” contributes to the elevated blood pressure and SND in sleep apnea patients (6, 40).

Analysis of mEPSCs provides insight into the quantal nature of glutamatergic synaptic transmission. We focused on AMPA receptors as mEPSCs are abolished by AMPA receptor

antagonists (74, 75). A change in mEPSC amplitude reflects alterations in the post-synaptic mechanisms of glutamatergic synaptic transmission, while changes in mEPSC frequency reflect alterations in transmitter release. mEPSCs could reflect spontaneous glutamate release from inputs arising from arterial chemoreceptor afferents and inputs arising from other central sites and/or local interneurons. CIH induced enhancement of mEPSC amplitude, with no change in frequency, may reflect enhanced sensitivity to glutamatergic inputs arising from any or all of these sources.

Post-synaptic factors that could lead to an increase in mEPSC amplitude include AMPA receptor sensitivity and receptor density. Our previous study found exposure to CIH did not alter the desensitization properties of AMPA receptors, eliminating this as a possible factor (12).  $\Delta$ FosB has been shown to increase transcription of GluR2 in reward pathways (46). Our group has observed increased expression of AMPA receptor GluR2 subunit, but not GluR1 subunit, in the NTS after chronic sustained hypoxia (74) and after CIH exposure (Bathina, Wu and Mifflin, unpublished observations). In addition to alterations in AMPA receptor levels due to changes in expression and/or degradation, receptor trafficking and/or post-translational modification (e.g. phosphorylation) of AMPA receptors could contribute to CIH-induced increase in responses to AMPA receptor activation.

Therefore, it is possible that the responses to spontaneous release of glutamate may exhibit increased amplitudes but this is not observed during synchronous electrical activation of all tractus inputs due to a decrease in the number of active synapses (2). Alternatively, spontaneously released glutamate may arise from synapses distinct from those formed by the tractus. Evoked and spontaneous glutamate release exhibit different characteristics and mEPSCs and eEPSCs can be differentially regulated (15, 27). Spontaneous release of glutamate has been

proposed as a mechanism that regulates basal excitability (27) so increased responses to spontaneous glutamate could increase discharge in response to activation of tractus-evoked inputs, even if the tractus-evoked inputs are reduced following exposure to CIH.

We found that within 1 day of exposure CIH, the amplitude of mEPSCs were enhanced. This suggests that the mechanisms mediating the CIH-induced persistent increase in MAP and SND are activated quite early by intermittent hypoxia. It would be interesting to determine if the initial responses to CIH have a similar basis as the long-lasting increase in MAP, SND and phrenic nerve discharge observed after acute ( $\leq 1$ hr) exposures to intermittent hypoxia in rats (14, 71, 72) and humans (11, 69).

Transcription factor  $\Delta$ FosB  $\Delta$ FosB is a member of the AP-1 family of transcription factors which includes cFos, FosB,  $\Delta$ FosB and the Fos-related antigens 1 (Fra1), and Fra2 (42-44, 46). Each of these species has its own time course of expression in response to acute, chronic or intermittent stimuli. Among these transcription factors, the truncated spliced isoform  $\Delta$ FosB has stable expression which persists for several days, making it a potentially important factor in the induction and maintenance of long-term plasticity following chronic, intermittent stimulation.  $\Delta$ FosB has been used as an effective marker of neuronal activation in response to wide range of stimuli such as stress, drug addiction, substance abuse (43, 46) and CIH (4, 9, 29). As a transcription factor,  $\Delta$ FosB regulates transcription of target genes such as GluR2, cyclin-dependent kinase 5 and NF-kB in the nucleus accumbens after chronic cocaine treatment (45). Cunningham et al. identified that in the median pre-optic nucleus CIH induces  $\Delta$ FosB which regulates expression of mitogen activated protein kinase kinase kinase 3, angiotensin converting enzymes (ACE1, ACE2) and nitric oxide synthase (nos1 and nos3) (9).  $\Delta$ FosB can also regulate

the expression of tyrosine hydroxylase (65), and our group recently reported catecholaminergic NTS neurons play a role in CIH induced hypertension (4).

We observed that CIH increased the number of  $\Delta$ FosB immunoreactive neurons in NTS within 1 day throughout 7 days CIH exposure. Within 1 day after the last exposure to CIH the number of  $\Delta$ FosB immunoreactive neurons in caudal and sub-postremal NTS were no different compared to levels observed under normoxic conditions. The amplitude of mEPSCs recorded from second order NTS neurons was significantly increased after 1 day CIH and 1 day CIH induces a persistent elevation in MAP (4, 23, 29). Furthermore, during normoxic recovery, MAP remains significantly elevated for 1-2 days, and the enhanced mEPSCs did not return to control levels until 3 days of recovery.  $\Delta$ FosB returns to control within 1 day after CIH whereas mEPSC amplitude remains increased for up to 3 days recovery from CIH suggesting that  $\Delta$ FosB induces changes that persist beyond the presence of the transcription factor. Taken together, these results suggest a relationship between  $\Delta$ FosB, mEPSC amplitude and CIH induced hypertension.

Catecholaminergic NTS neurons play an important role in stress responses (59) and contribute to the effects of CIH on autonomic and endocrine functions to increase MAP (4) by enhanced sympathetic outflow and/or by up-regulation of the hypothalamic–pituitary–adrenal axis (7, 35) as well as other mechanisms. Our previous work demonstrated that catecholaminergic NTS neurons express  $\Delta$ FosB following a 7 day exposure to CIH (29). Our present study extends this observation by examining  $\Delta$ FosB during shorter exposures to CIH. We found no significant changes in the number of catecholaminergic NTS neurons exhibiting  $\Delta$ FosB immunoreactivity following CIH exposures of less than 7 days. This contrasts with the temporal pattern of  $\Delta$ FosB observed in non-catecholaminergic NTS neurons where the number of NTS neurons exhibiting  $\Delta$ FosB immunoreactivity was increased after 1 day of CIH.

To further elucidate the functional role of  $\Delta$ FosB in the CIH-induced changes in glutamatergic transmission, we blocked the transcriptional function of  $\Delta$ FosB in the NTS using a dominant negative AAV-GFP- $\Delta$ JunD construct. We then examined changes in AMPA receptor mediated mEPSCs in second order NTS neurons. We found that the increase in mEPSC amplitude induced by 1 day and 7 days CIH was eliminated after functionally blocking  $\Delta$ FosB in NTS. The dominant-negative construct eliminated the CIH induced reduction in eEPSC amplitude. Differential regulation of spontaneous vs. evoked transmitter release has been reported and the factors mediating CIH- $\Delta$ FosB enhancement of mEPSCs might not be present at synapses receiving tractus evoked inputs.

Increased glutamatergic inputs from chemoreceptors and increased sensitivity to glutamatergic inputs leading to increased NTS neuron discharge during CIH could be the signal that reduces the number of active synapses. Inhibition of  $\Delta$ FosB eliminated both the CIH-induced increase in mEPSC amplitude and the CIH-induced decrease in the amplitude of the tractus-eEPSC. While the summed response generated by synchronous activation of all tractus inputs may be reduced following CIH due to a reduction in the number of active synapses, the responses to activation of a single input may be enhanced. Also, keep in mind that in vivo NTS neurons are not exposed to synchronous activation of all tractus inputs but rather an afferent volley of afferent inputs dispersed in time by differences in threshold, conduction velocity.

In conclusion, CIH increases the post-synaptic response to spontaneous synaptic release of glutamate and this increase occurs quite rapidly, within 1 day of CIH exposure. This increase follows the same time course as expression of  $\Delta$ FosB in the NTS following CIH exposure and can be blocked by interfering with the function of  $\Delta$ FosB. CIH increases the number of NTS neurons expressing  $\Delta$ FosB immunoreactivity, through which the effect of arterial chemoreceptor

glutamatergic synaptic inputs to second order NTS neurons is enhanced. This provides evidence for augmented signaling capacity from these neurons to sympatho-excitatory sites to increase SND and arterial pressure. A better understanding of the underlying mechanisms of the pathogenesis and maintenance of CIH hypertensive mechanisms may provide us with a better understanding of systemic hypertension in sleep apnea patients and guide future mechanism based clinical treatments.

### **Acknowledgments**

The authors gratefully acknowledge the financial support of NIH (HL PO1-088052) and American Heart Association Pre-Doctoral Fellowship (13PRE16970013). The authors gratefully acknowledge Dr. Eric Nestler, Mount Sinai School of Medicine, for providing the dominant-negative and overexpression viral constructs.

## **Figure Legends**

Figure 1. Representative digital images of  $\Delta$ FosB (A, B) and DBH (C, D) immunostaining and co-localization (E, F:  $\Delta$ FosB is pseudo-colored green, DBH is colored red) in the NTS from a control rat (left column) and a 7 day CIH rat (right column). Red arrows indicate a few of the cells with co-immunoreactivity for  $\Delta$ FosB and DBH . cc = central canal. Scale bar: 100  $\mu$ m

Figure 2. A. The number of  $\Delta$ FosB immunoreactive neurons (A) and  $\Delta$ FosB+DBH (B) immunoreactive neurons in NTS in control (n=14), 1 day CIH (n=7), 3 days CIH (n=7), 5 days CIH (n=7), 7 days CIH (n=17) and 1 day recovery (n=6), 3 days recovery (n=5), 7 days recovery (n=2) groups. \* =  $p \leq 0.05$  vs. control by one-way ANOVA with Dunn' s post-hoc analysis.

Figure 3. Effect of CIH on mEPSCs. A, B. Whole-cell patch-clamp recording from second-order arterial chemoreceptor neurons in the NTS. The cell indicated by the arrow in A (differential infrared contrast DIC) exhibited DiA immunofluorescence in B. C. Recordings of mEPSCs from a neuron in control (No CIH) group (upper sweep) and from a neuron in 1 day CIH group (lower sweep). All data were collected in the presence of the sodium channel blocker TTX (0.5  $\mu$ M) and GABA<sub>A</sub> receptor antagonist gabazine (25  $\mu$ M). D. Cumulative probabilities of the amplitude (left) and inter event interval (right) under no CIH and during CIH in the same neuron as illustrated in A and B.

Figure 4. Effect of different duration CIH exposures on mEPSC amplitude (A) and frequency (B). CIH 1 day (n=11), 3 day (n=11), 5 day (n=21), 7 day (n=7), and CIH 7 day+1 day recovery

(n=4) increased the amplitude of mEPSCs compared with control (no CIH, n=12).  $* = p \leq 0.05$  vs. control by one-way ANOVA with SNK post-hoc analysis. Frequencies were not significantly different in all groups.

Figure 5. Effect of dominant negative (dn) blockade of  $\Delta$ FosB on mEPSCs. A. Green fluorescent protein (GFP) labeling following injection of dominant-negative construct into the NTS. cc = central canal. B. mEPSCs from neurons exhibiting GFP and DiA labeling. Sweeps from top to bottom: CIH 1 Day; CIH 1 Day dn; CIH 7 Day; CIH 7 Day dn. C. Mean data from groups; histogram bars from left to right: mEPSC amplitude from control (no CIH, n=12), CIH 1 Day (n=11), CIH 1 D sham (n=17), CIH 1 D dn (n=10), CIH 7 Day (n=7), CIH 7 D sham (n=18), CIH 7 D dn (n=19) groups.  $* = p < 0.01$  vs. control;  $\# = p < 0.01$  vs. CIH 1 Day;  $\#\# = p < 0.05$  vs. CIH 1 D sham.  $** = p < 0.01$  vs. CIH 7 Day.  $*** = p < 0.001$  vs. CIH 7 D sham. One-way ANOVA with SNK post-hoc analysis.

Figure 6. Effect of dominant negative (dn) blockade of  $\Delta$ FosB on tractus eEPSCs. A: Each panel is an average of 7-10 responses generated by 0.5Hz tractus stimulation. Top to bottom: neuron from rat injected with the sham dominant-negative construct and maintained in normoxic conditions; neuron from rat exposed to 7 days CIH; neuron from rat which received an NTS injection of the dn construct prior to a 7 day exposure to CIH. B. Mean data for population.  $* = p < 0.05$ . One-way ANOVA with SNK post-hoc analysis.

Figure 7. Effect of over-expression of  $\Delta$ FosB on mEPSCs. A. Sweeps from top to bottom illustrate mEPSCs from a: neuron in the control, normoxia group; in the CIH 7 Day exposure

group; neuron labeled with GFP in  $\Delta$ FosB overexpression group (no CIH exposure); neuron in  $\Delta$ FosB overexpression group with no GFP labeling. B. Mean data of mEPSC amplitude from control (n=12), CIH 7 Day (n=7),  $\Delta$ FosB overexpression (n=10) and  $\Delta$ FosB overexpression non-GFP (n=13) groups. \* = p < 0.001 vs. control; # = p < 0.01 vs.  $\Delta$ FosB overexpression; ## = p < 0.05 vs. CIH 7 Day. One-way ANOVA with SNK post-hoc analysis.

## **References**

1. **Ainslie PN, Barach A, Cummings KJ, Murrell C, Hamlin M, and Hellemans J.** Cardiorespiratory and cerebrovascular responses to acute poikilocapnic hypoxia following intermittent and continuous exposure to hypoxia in humans. *J Appl Physiol* 102: 1953-1961, 2007.
2. **Almado CEL, Machado BH, and Leao RM.** Chronic intermittent hypoxia depresses afferent neurotransmission in NTS neurons by a reduction in the number of active synapses. *J Neurosci* 32: 16737-16746, 2012.
3. **Bailey TW, Hermes SM, Andresen MC, and Aicher SA.** Cranial visceral afferent pathways through the nucleus of the solitary tract to caudal ventrolateral medulla or paraventricular hypothalamus: Target-specific synaptic reliability and convergence patterns. *J Neurosci* 26: 11893-11902, 2006.
4. **Bathina CS, Rajulapati A, Franzke M, Yamamoto K, Cunningham JT, and S.W. M.** Knockdown of tyrosine hydroxylase in the nucleus of the solitary tract reduces elevated blood pressure during chronic intermittent hypoxia. *Am J Physiol* 305: R1031-R1039, 2013.
5. **Bratel T, Wennlund A, and Carlstrom K.** Pituitary reactivity, androgens and catecholamines in obstructive sleep apnoea. Effects of continuous positive airway pressure treatment (CPAP). *Resp Med* 93: 1-7, 1999.

6. **Carlson J.T., Hedner J., Elam M., Ejnell H., Sellgren J., and B.G. W.** Augmented resting sympathetic activity in awake patients with obstructive sleep apnea. *Chest* 103: 1763-1768, 1993.
7. **Chintamaneni K, Bruder ED, and Raff H.** Effects of age on ACTH, corticosterone, glucose, insulin and mRNA levels during intermittent hypoxia in the neonatal rat. *Am J Physiol Regul Integr Comp Physiol* 304: R782-R789, 2013.
8. **Costa-Silva JH, Zoccal DB, and Machado BH.** Chronic intermittent hypoxia alters glutamatergic control of sympathetic and respiratory activities in the commissural NTS of rats. *Am J Physiol Regul Integr Comp Physiol* 302: R785-R793, 2012.
9. **Cunningham JT, Knight WD, Chakravarty S, Mifflin SW, and Nestler EJ.** An essential role for  $\Delta$ FosB in the median preoptic nucleus in the sustained hypertensive effects of intermittent hypoxia. *Hypertension* 60: 179-187, 2012.
10. **Cutler MJ, Swift NM, Keller DM, Wasmund WL, Burk JR, and Smith ML.** Periods of intermittent hypoxic apnea can alter chemoreflex control of sympathetic nerve activity in humans. *American Journal of Physiology - Heart & Circulatory Physiology* 287: H2054-2060, 2004.
11. **Cutler MJ, Swift NM, Keller DM, Wasmund WL, and Smith ML.** Hypoxia-mediated prolonged elevation of sympathetic nerve activity after periods of intermittent hypoxia. *J Appl Physiol* 96: 754-761, 2004.

12. **de Paula PM, Tolstykh G, and Mifflin SW.** Chronic intermittent hypoxia alters NMDA and AMPA evoked currents in NTS neurons receiving carotid body chemoreceptor inputs. *Am J Physiol* 292: R2259-R2265, 2007.
13. **Dempsey JA, Veasey SC, Morgan BJ, and O'Donnell CP.** Pathophysiology of sleep apnea. *Physiol Rev* 90: 47-112, 2010.
14. **Dick TE, Hsieh YH, Wang N, and Prabhakar N.** Acute intermittent hypoxia increases both phrenic and sympathetic nerve activities in the rat. *Experimental Physiology* 92: 87-97, 2007.
15. **Fawley JA, Hofmann ME, and Andresen MC.** Cannabinoid 1 and transient receptor potential vanilloid 1 receptors discretely modulate evoked glutamate separately from spontaneous glutamate transmission. *J Neurosci* 34: 8324-8322, 2014.
16. **Fletcher EC.** Sympathetic over activity in the etiology of hypertension of obstructive sleep apnea. *Sleep* 26: 15-19, 2003.
17. **Fletcher EC, Lesske J, Behm R, Miller CC, 3rd, Stauss H, and Unger T.** Carotid chemoreceptors, systemic blood pressure, and chronic episodic hypoxia mimicking sleep apnea. *J Appl Physiol* 72: 1978-1984, 1992.
18. **Fletcher EC, Lesske J, Qian W, Miller CC, and Unger T.** Repetitive, episodic hypoxia causes diurnal elevation of blood pressure in rats. *Hypertension* 19: 555-561, 1992.
19. **Foster GE, Brugniaux JV, Pialoux V, Duggan CTC, Hanly PJ, Ahmed SB, and Poulin MJ.**

Cardiovascular and cerebrovascular responses to acute hypoxia following exposure to intermittent hypoxia in healthy humans. *J Physiol* 587: 3287-3299, 2009.

20. **Greenberg HE, Sica A, Batson D, and Scharf SM.** Chronic intermittent hypoxia increases sympathetic responsiveness to hypoxia and hypercapnia. *J Appl Physiol* 86: 298-305, 1999.
21. **Greenberg HE, Sica AL, Scharf SM, and Ruggiero DA.** Expression of c-fos in the rat brainstem after chronic intermittent hypoxia. *Brain Res* 816: 638-645, 1999.
22. **Guyenet PG.** Neural structures that mediate sympathoexcitation during hypoxia. *Respiration Physiology* 121: 147-162, 2000.
23. **Hinojosa-Laborde C and Mifflin SW.** Sex differences in blood pressure response to intermittent hypoxia in rats. *Hypertension* 46: 1016-1021, 2005.
24. **Huang J, Lusina S, Xie T, Ji E, Xiang S, Liu Y, and Weiss JW.** Sympathetic response to chemostimulation in conscious rats exposed to chronic intermittent hypoxia. *Resp Physiol and Neurobiol* 166: 102-106, 2009.
25. **Imadojemu VA, Mawji Z, Kunselamn A, Gray KS, Hogeman CS, and Leuenberger UA.** Sympathetic chemoreflex responses in obstructive sleep apnea and effects of continuous positive airway pressure therapy. *Chest* 131: 1406-1413, 2007.
26. **Kapa S, Kuniyoshi FHS, and Somers V.** Sleep apnea and hypertension: Interactions and implications for management. *Hypertension* 51: 605-608, 2008.
27. **Kavalali ET.** The mechanisms and functions of spontaneous neurotransmitter release. *Nature Reviews Neuroscience* 16: 5-16, 2015.

28. **Kline D, Ramirez-Navarro A, and Kunze DL.** Adaptive depression in synaptic transmission in the nucleus of the solitary tract after in vivo chronic intermittent hypoxia: Evidence for homeostatic plasticity. *J Neurosci* 27: 4663-4673, 2007.
29. **Knight WD, Little JT, Carreno FR, Toney GM, Mifflin SW, and Cunningham JT.** Chronic intermittent hypoxia increases blood pressure and expression of FosB/deltaFosB in central autonomic regions. *Am J Physiol Regul Integr Comp Physiol* 301: R131-R139, 2011.
30. **Knight WD, Saxena A, Shell B, Nedungadi TP, Mifflin SW, and Cunningham JT.** Central losartan attenuates increases in arterial pressure and expression of FosB/deltaFosB along the autonomic axis associated with chronic intermittent hypoxia. *Am J Physiol Reg Integr Comp* 305: R1051-1058, 2013.
31. **Konecny T, Kara T, and Somers V.** Obstructive sleep apnea and hypertension: An update. *Hypertension* 63: 203-209, 2014.
32. **Kushida CA, Chediak A, Berry RB, Brown LK, Gozal D, Iber C, Parthasarathy S, Quan SF, Rowley JA, Positive Airway Pressure Titration Task F, and American Academy of Sleep M.** Clinical guidelines for the manual titration of positive airway pressure in patients with obstructive sleep apnea. *Journal of Clinical Sleep Medicine* 4: 157-171, 2008.
33. **Lesske J, Fletcher EC, Bao G, and Unger T.** Hypertension caused by chronic intermittent hypoxia-influence of chemoreceptors and sympathetic nervous system. *J Hypertens* 15: 1593-1603, 1997.

34. **Leuenberger UA, Hogeman CS, Quraishi S, Linton-Frazier L, and Gray KS.** Short-term intermittent hypoxia enhances sympathetic responses to continuous hypoxia in humans. *J Appl Physiol* 103: 835-842, 2007.
35. **Ma S, Mifflin SW, Cunningham JT, and Morilak DA.** Chronic intermittent hypoxia sensitizes acute hypothalamic-pituitary-adrenal stress reactivity and Fos induction in the rat locus coeruleus in response to subsequent immobilization stress. *Neuroscience* 154: 1639-1647, 2008.
36. **McClung CA, Ulery PG, Perrotti L, Zachariou V, Berton O, and Nestler EJ.** DeltaFosB: a molecular switch for long-term adaptation in the brain. *Mol Br Res* 132: 146-154, 2004.
37. **McNicholas WT.** Cardiovascular outcomes of CPAP therapy in obstructive sleep apnea syndrome. *Am J Physiol (Reg Int Comp Physiol)* 293: R1666-R1670, 2007.
38. **Mendelowitz D, Yang M, Andresen MC, and Kunze DL.** Localization and retention in vitro of fluorescently labeled aortic baroreceptor terminals on neurons from the nucleus tractus solitarius. *Brain Research* 581: 339-343, 1992.
39. **Narkiewicz K and Somers V.** The sympathetic nervous system and obstructive sleep apnea. *J Hypertens* 15: 1613-1619, 1997.
40. **Narkiewicz K, van de Borne PJ, Montano N, Dyken ME, Phillips BG, and Somers VK.** Contribution of tonic chemoreflex activation to sympathetic activity and blood pressure in patients with obstructive sleep apnea. *Circulation* 97: 943-945, 1998.

41. **Narkiewicz K, van de Borne PJ, Pesek CA, Dyken ME, Montano N, and Somers VK.** Selective potentiation of peripheral chemoreflex sensitivity in obstructive sleep apnea. *Circulation* 99: 1183-1189, 1999.
42. **Nestler EJ.** Is there a common molecular pathway for addiction? *Nat Neurosci* 8: 1145-1149, 2005.
43. **Nestler EJ.** Molecular basis of long-term plasticity underlying addiction. *Nat Rev Neurosci* 2: 119-128, 2001.
44. **Nestler EJ.** Molecular neurobiology of addiction. *Am J Addiction* 10: 201-217, 2001.
45. **Nestler EJ.** Transcriptional mechanisms of addiction: role of delta FosB. *Philos Trans R Soc Lond B Biol Sci* 363: 3245-3255, 2008.
46. **Nestler EJ, Barrot M, and Self DW.** DeltaFosB: a sustained molecular switch for addiction. *Proc Natl Acad Sci* 98: 11042-11046, 2001.
47. **Nye HE and Nestler EJ.** Induction of chronic Fos-related antigens in rat brain by chronic morphine administration. *Mol Pharmacol* 49: 636-645, 1996.
48. **Olivan MV, Bonagamba LG, and Machado BH.** Involvement of the paraventricular nucleus of the hypothalamus in the pressor response to chemoreflex activation in awake rats. *Brain Research* 895: 167-172, 2001.
49. **Paxinos G and Watson C.** *The Rat Brain in Stereotaxic Coordinates*, 6th Edition: Academic Press, 2006.

50. **Peng Y-J, Overholt JL, Kline D, Kumar GK, and Prabhakar NR.** Induction of sensory long-term facilitation in the carotid body by intermittent hypoxia: Implications for recurrent apneas. *PNAS* 100: 10073-10078, 2003.
51. **Peng Y-J and Prabhakar NR.** Effects of two paradigms of chronic intermittent hypoxia on carotid body sensory activity. *J Appl Physiol* 96: 1236-1242, 2003.
52. **Peng Y-J, Yuan G, Khan S, Nanduri J, Makarenko VV, Reddy VD, Vasavda C, Kumar GK, Semenza GL, and Prabhakar NR.** Regulation of hypoxia-inducible factor- $\alpha$  isoforms and redox state by carotid body neural activity in rats. *J Physiol* 592: 3841-3858, 2014.
53. **Peng Y, Kline DD, Dick TE, and Prabhakar NR.** Chronic intermittent hypoxia enhances carotid body chemoreceptor response to low oxygen. *Advances in Experimental Medicine & Biology* 499: 33-38, 2001.
54. **Prabhakar NR, Dick TE, Nanduri J, and Kumar GK.** Systemic, cellular and molecular analysis of chemoreflex-mediated sympathoexcitation by chronic intermittent hypoxia. *Experimental Physiology* 92: 39-44, 2007.
55. **Prabhakar NR, Peng YJ, Jacono FJ, Kumar GK, and Dick TE.** Cardiovascular alterations by chronic intermittent hypoxia: importance of carotid body chemoreflexes. *Clinical & Experimental Pharmacology & Physiology* 32: 447-449, 2005.
56. **Ramirez J-M, Garcia III AJ, Anderson TM, Koschnitzky JE, Peng Y-J, Kumar GK, and Prabhakar NR.** Central and peripheral factors contributing to obstructive sleep apneas. *Resp Physiol and Neurobiol* 189: 344-353, 2013.

57. **Reddy MK, Patel KP, and Schultz HD.** Differential role of the paraventricular nucleus of the hypothalamus in modulating the sympathoexcitatory component of peripheral and central chemoreflexes. *Am J Physiol* 289: R789-R797, 2005.
58. **Reeves SR, Gozal E, Guo SZ, Sachleben Jr. LR, Brittian KR, Lipton AJ, and Gozal D.** Effect of long term intermittent and sustained hypoxia on hypoxic ventilatory and metabolic responses in the adult rat. *J Appl Physiol*, 2003.
59. **Rinaman L.** Hindbrain noradrenergic A2 neurons: diverse roles in autonomic, endocrine, cognitive, and behavioral functions. *Am J Physiol Regul Integr Comp Physiol* 300: R22-R235, 2011.
60. **Saarelainen S, Hasan J, SSiitonen S, and Seppala E.** Effect of nasal CPAP treatment on plasma volume, aldosterone and 24-h blood pressure in obstructive sleep apnea. *J Sleep Res* 5: 181-185, 1996.
61. **Shamsuzzaman AS, Gersh BJ, and Somers V.** Obstructive sleep apnea: Implications for cardiac and vascular disease. *J Amer Med Assoc* 290: 1906-1914, 2003.
62. **Sharpe AL, Calderon AS, Andrade MA, Cunningham JT, Mifflin SW, and Toney GM.** Chronic intermittent hypoxia increases sympathetic control of blood pressure: role of neuronal activity in the hypothalamic paraventricular nucleus. *Am J Physiol* 305: H1772-H1780, 2013.
63. **Silva AQ and Schreihof AM.** Altered sympathetic reflexes and vascular reactivity in rats after exposure to chronic intermittent hypoxia. *J Physiol* 589: 1463-1476, 2011.

64. **Somers VK, Dyken ME, Clary MP, and Abboud FM.** Sympathetic neural mechanisms in obstructive sleep apnea. *J Clin Invest* 96: 1897-1904, 1995.
65. **Teegarden SL, Nestler EJ, and Bale TL.** DeltaFosB-mediated alterations in dopamine signaling are normalized by a palatable high-fat diet. *Biol Psychiatry* 64: 941-950, 2008.
66. **Turovskayaa MV, Turovskya EA, Zinchenkoa VP, Levin SG, Shamsutdinova AA, and Godukhinb OV.** Repeated brief episodes of hypoxia modulate the calcium responses of ionotropic glutamate receptors in hippocampal neurons. *Neurosci Lett* 496: 11-14, 2011.
67. **Turrigiano GG.** Homeostatic plasticity in neuronal networks: The more things change, the more they stay the same. *Trends in Neuroscience* 22: 221-227, 1999.
68. **Vardhan A, Kachroo A, and Sapru H.** Excitatory amino acid receptors in the commissural nucleus of the NTS mediate carotid chemoreceptor responses. *Am J Physiol (Reg Int Comp)* 264: R41-R50, 1993.
69. **Xie A, Skatrud JB, Puleo DS, and Morgan BJ.** Exposure to hypoxia produces long-lasting sympathetic activation in humans. *J Appl Physiol* 91: 1555-1562, 2001.
70. **Xie W, Zheng F, and Song X.** Obstructive sleep apnea and serious adverse outcomes in patients with cardiovascular or cerebrovascular disease: A PRISMA-compliant systematic review and meta analysis. *Medicine* 93: 1-8, 2014.
71. **Xing T and Pilowsky PM.** Acute intermittent hypoxia in rat in vivo elicits a robust increase in tonic sympathetic nerve activity that is independent of respiratory drive. *J Physiol* 588: 3075-3088, 2010.

72. **Yamamoto K, Lalley P, and Mifflin S.** Acute intermittent optogenetic stimulation of nucleus tractus solitarius neurons induces sympathetic long-term facilitation. *Am J Physiol Regul Integr Comp Physiol* 308: R266-R275, 2015.
73. **Zachariou V, Bolanos CA, Selley DE, Theobald D, Cassidy MP, Kelz MB, Shaw-Lutchman T, Berton O, Sim-Selley LJ, Dileone RJ, Kumar A, and Nestler EJ.** An essential role for DeltaFosB in the nucleus accumbens in morphine action. *Nat Neurosci* 9: 205-211, 2006.
74. **Zhang W, Carreno FR, Cunningham JT, and Mifflin SW.** Chronic sustained hypoxia enhances both evoked EPSCs and norepinephrine inhibition of glutamatergic afferent inputs in the nucleus of the solitary tract. *J Neurosci* 29: 3093-3102, 2009.
75. **Zhang W, Carreno FR, Cunningham JT, and Mifflin SW.** Chronic sustained and intermittent hypoxia reduce function of ATP-sensitive potassium channels in nucleus of the solitary tract. *Am J Physiol* 295: doi:10.1152/ajpregu.90390.92008, 2008.
76. **Zhang W and Mifflin SW.** Injections of kynurenic acid into the NTS attenuate cardiovascular responses to chemoreceptor activation in the rat. *Am J Physiol (Heart Circ)* 265: H770-H773, 1993.
77. **Zhang W and Mifflin SW.** Excitatory amino acid receptors within NTS mediate arterial chemoreceptor reflexes in rats. *Am J Physiol* 265: H770-773, 1993.
78. **Zoccal DB, Bonagamba LG, Oliveira FR, Antunes-Rodrigues J, and Machado BH.** Increased sympathetic activity in rats submitted to chronic intermittent hypoxia. *Experimental Physiology* 92: 79-85, 2007.

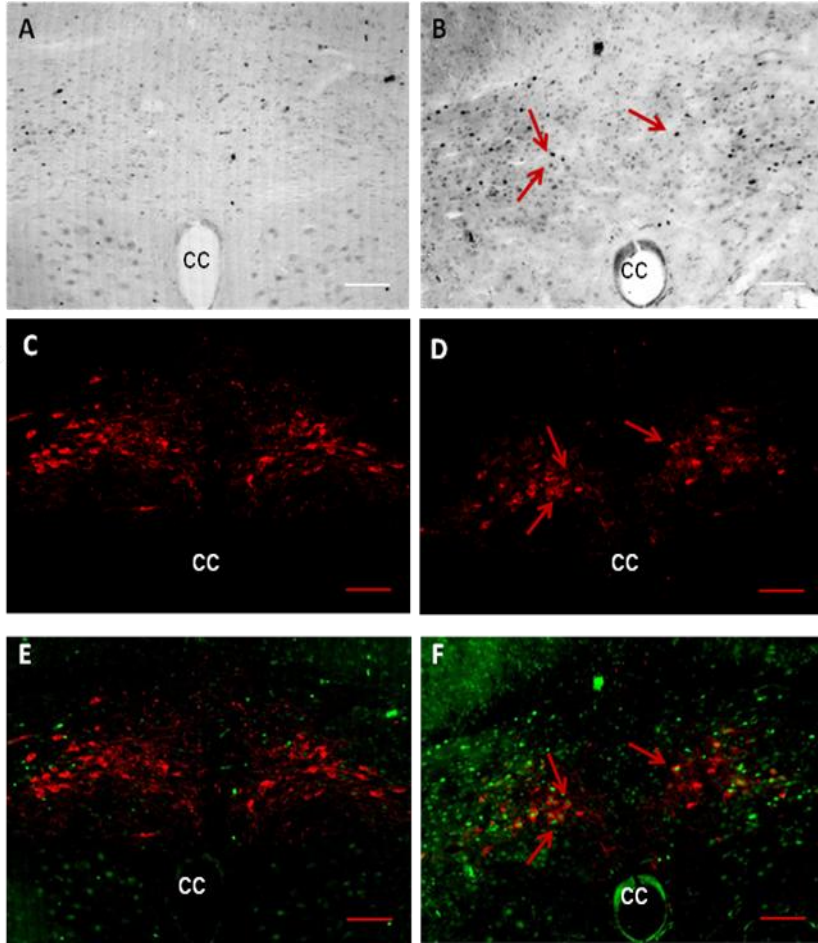


Figure 1

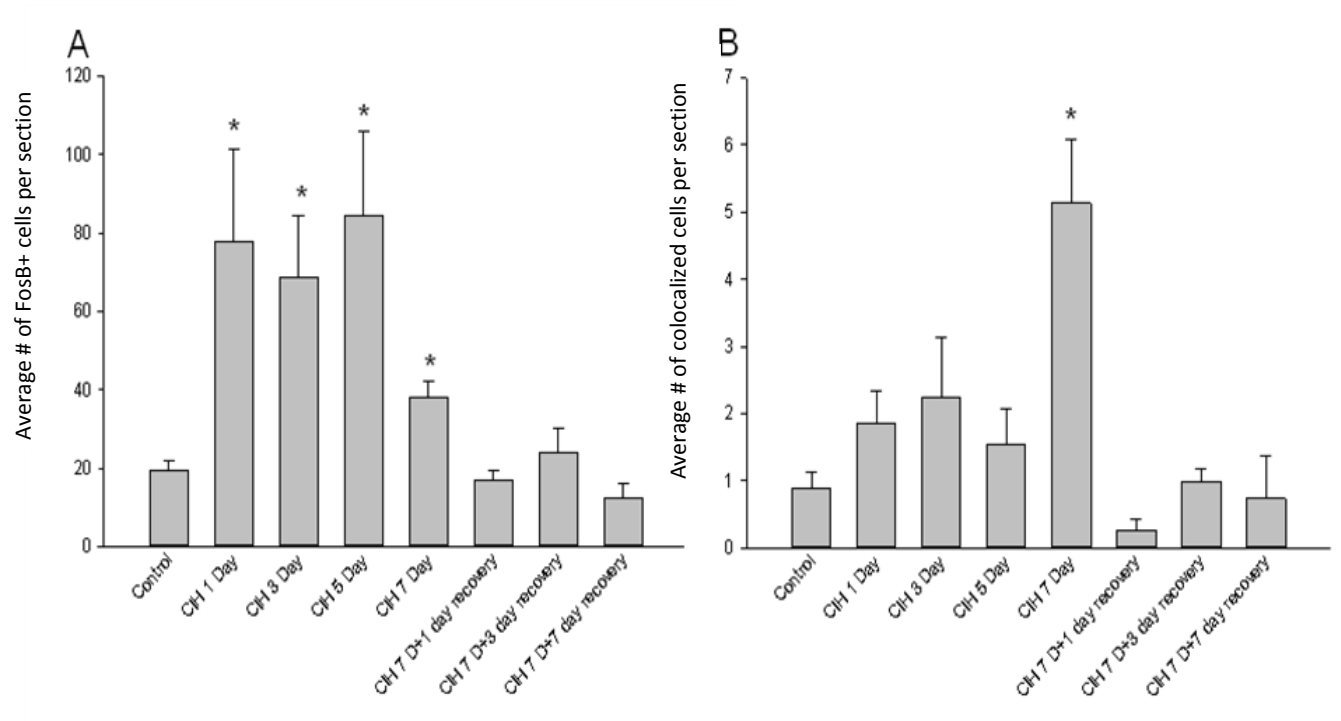


Figure 2

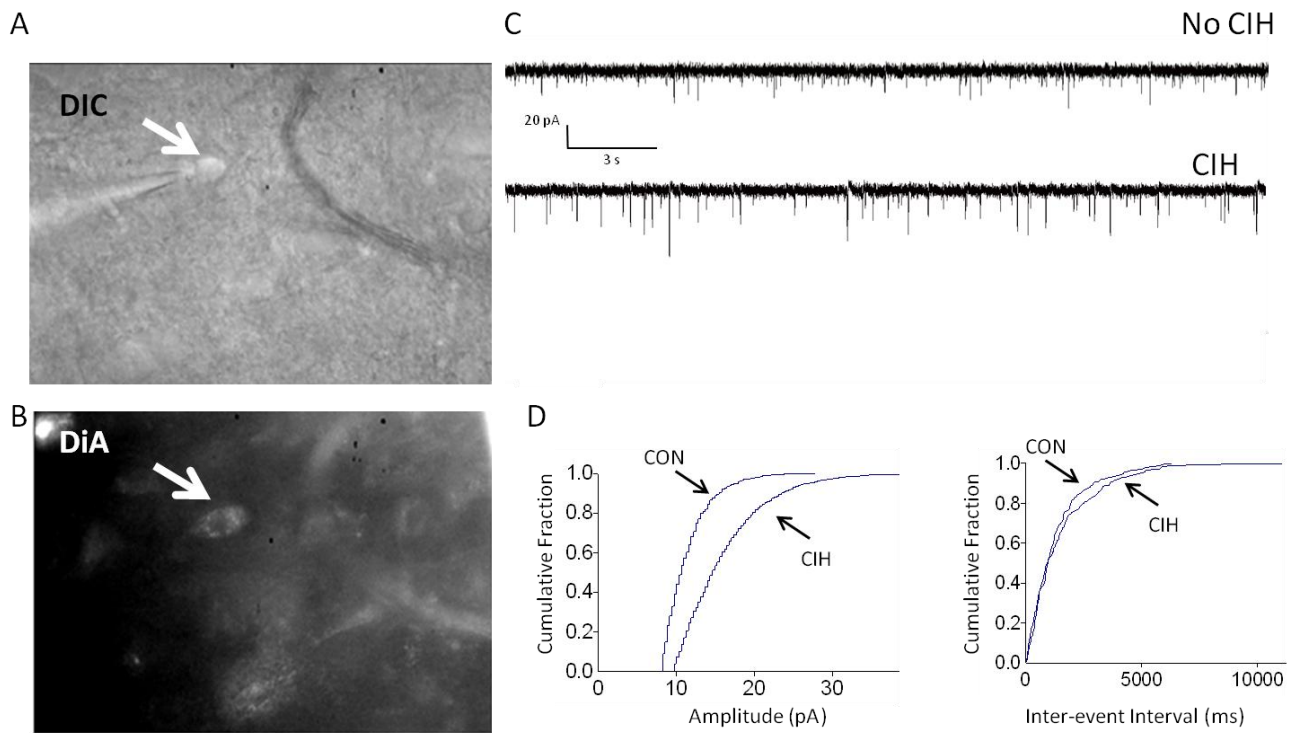


Figure 3

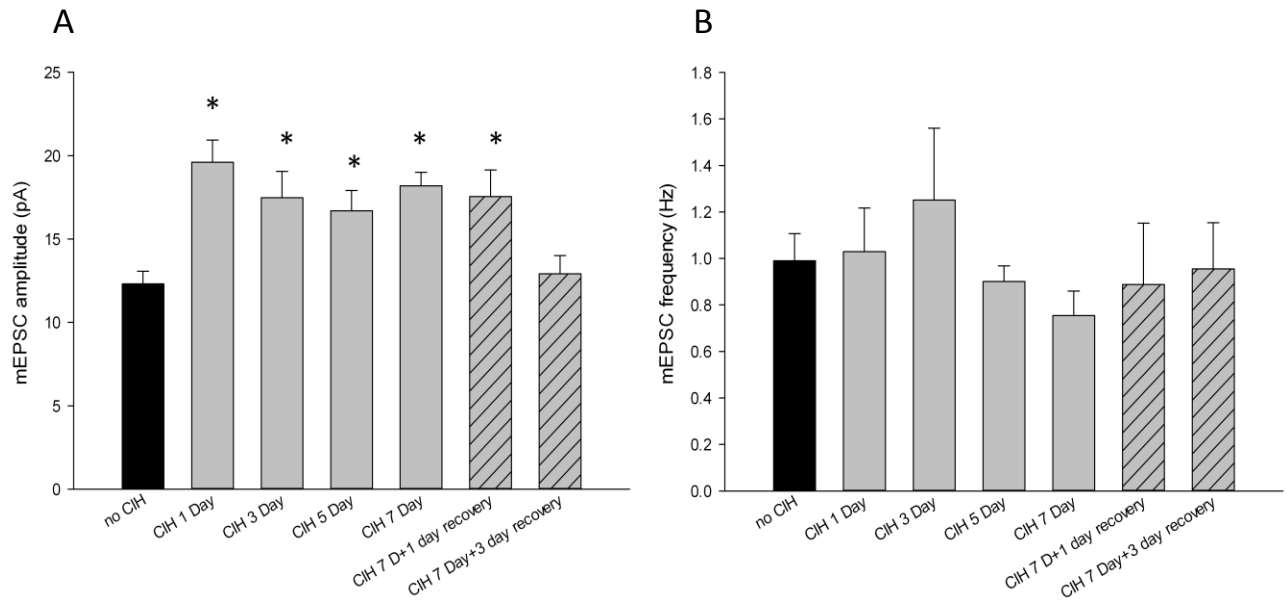


Figure 4

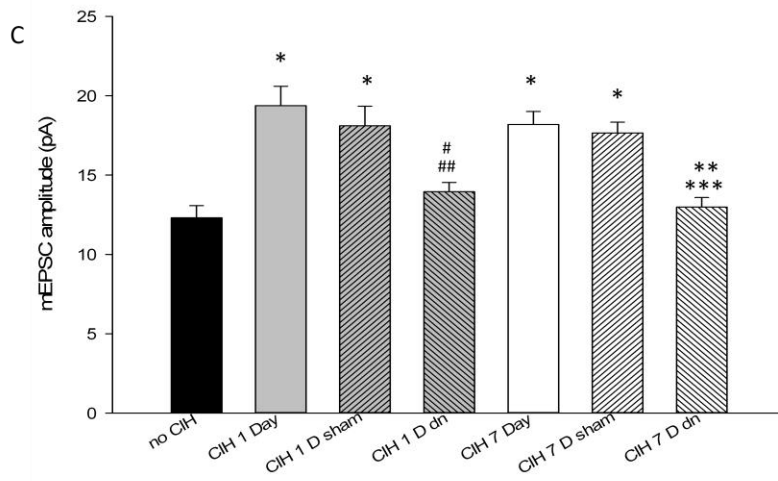
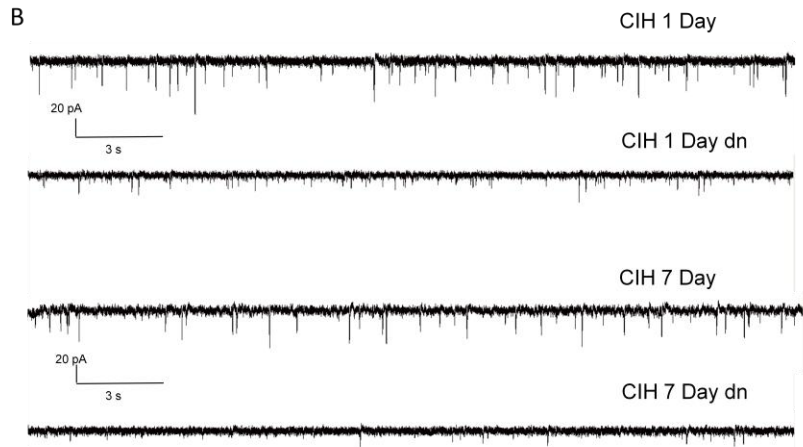
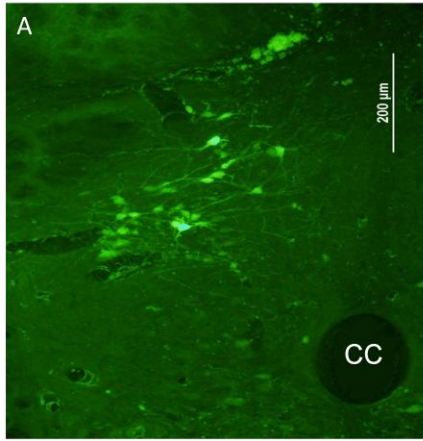


Figure 5

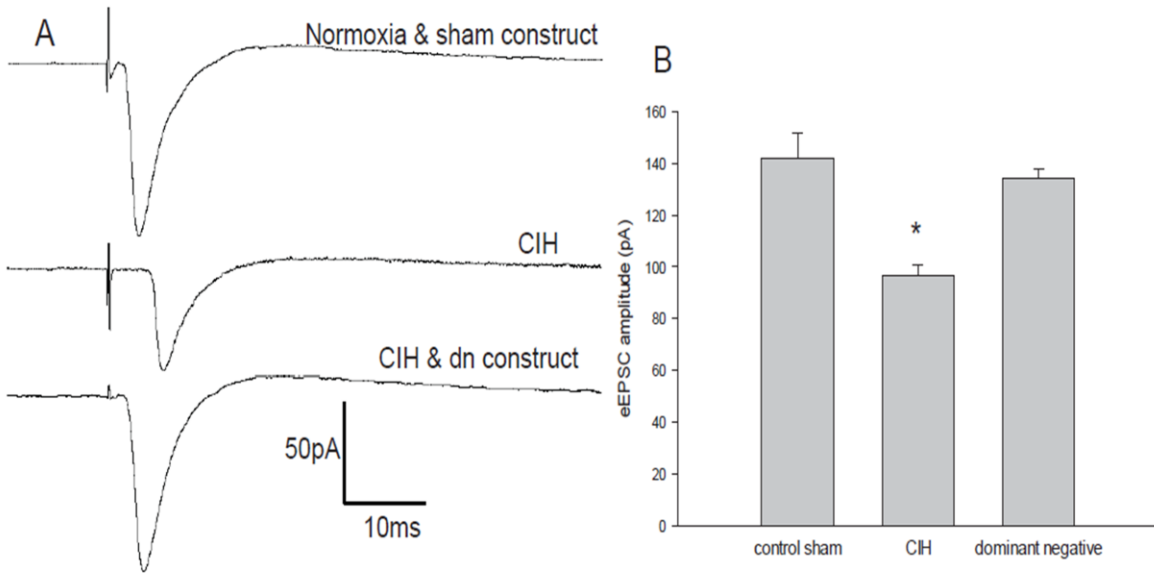


Figure 6

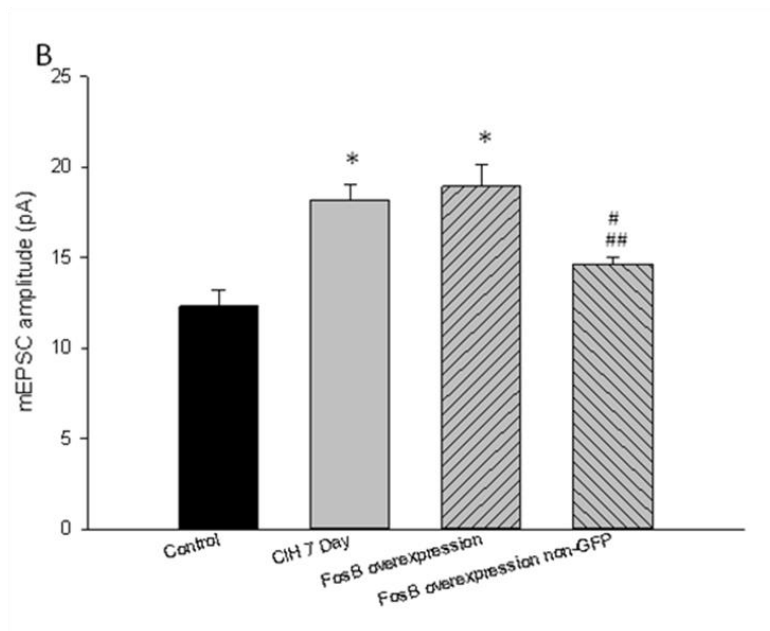
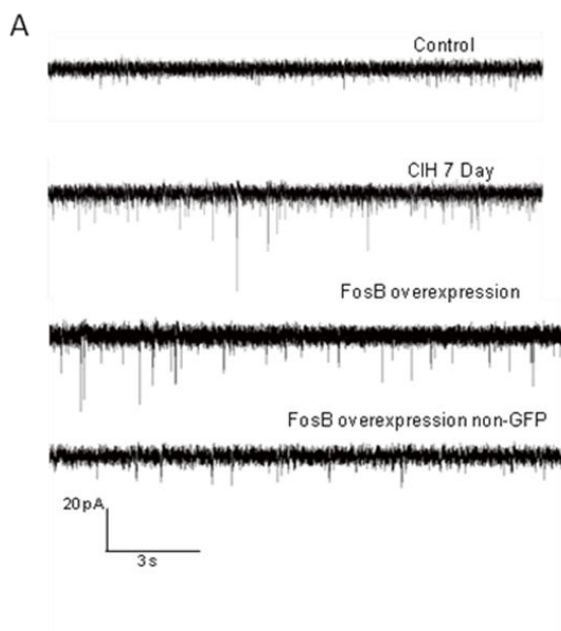


Figure 7

## CHAPTER IV

### **SUMMARY AND CONCLUSIONS**

The purpose of this study was to ascertain the role of transcription factor  $\Delta$ FosB in the NTS in regulation of cardiovascular and respiratory responses in rats exposed to CIH. The summary of results from the 3 specific aims represented as chapters II and III are:

1. It is possible to block function of  $\Delta$ FosB in the NTS through AAV delivery technique.
2.  $\Delta$ FosB blockade in the NTS reduces hypertension observed during CIH.
3.  $\Delta$ FosB blockade in the NTS reduces the excitatory drive to the PVN.
4. Time course of the development of  $\Delta$ FosB immunoreactivity is rapid, starting from one day CIH, lasting the entire seven days of CIH. Recovery from seven days CIH is also quick; one day normoxic recovery can fully reduce elevated  $\Delta$ FosB immunoreactivity back to control level.
5. Development of  $\Delta$ FosB immunoreactivity in catecholaminergic neurons is slower, with a significant increase observed only after seven days CIH.
6. Time course of changes in spontaneous glutamate synaptic transmission during different periods of CIH exposure is similar to the time course of  $\Delta$ FosB immunoreactivity. CIH increased mEPSC amplitude within one day of CIH, and this is maintained for seven days of CIH and one day recovery after seven days of CIH.

7. The CIH induced increase in mEPSC amplitude is mediated by  $\Delta$ FosB.
8.  $\Delta$ FosB can increase mEPSC amplitude without CIH exposure.
9.  $\Delta$ FosB also mediates reduction of tractus evoked glutamatergic transmission after seven days of CIH.

Based on these results, the first and foremost conclusion is that  $\Delta$ FosB in the NTS plays an important role in the sustained hypertension observed during CIH. Our overall hypothesis can be accepted based on these results and the series of events occurring during CIH could be:

**“Glutamate released from arterial chemoreceptor afferents due to hypoxemia activation during CIH can act through AMPA receptors on the second order NTS neurons to increase responses to spontaneous glutamate transmission. This event is mediated by NTS  $\Delta$ FosB. The resulting effect might be increased excitatory drive from the NTS neurons to the downstream sympetho-excitatory nuclei increases SNA and sustains hypertension during CIH”.**

## **LIMITATIONS AND FUTURE STUDIES**

Overall, this research increased our understanding of the mechanisms behind the hypertension observed during CIH. However, there are further studies that could be conducted based upon the results of this investigation. The following experiments are proposed:

1. Measuring the amount of neurotransmitter release at the upstream nuclei like PVN, MnPO and the downstream nuclei like RVLN after blockade of  $\Delta$ FosB in the NTS.
2. Corticosterone measurement in the AAV-GFP- $\Delta$ JunD injected rats after seven days of CIH.
3. To determine if  $\Delta$ FosB blockade in the NTS could decrease SNA in CIH exposed rats.
4. To measure the angiotensin concentration in AAV-GFP- $\Delta$ JunD injected rats after CIH exposure.
5. Protein analysis for both non-phosphorylated forms and phosphorylated forms of AMPA receptor subunits in NTS of CIH exposed rats.
6. Laser capture microdissection (LCM) measurement of mRNA levels of AMPA receptor subunits, NMDA receptor subunits and angiotensin receptors in AAV-GFP- $\Delta$ JunD injected neurons after seven days of CIH.
7. AMPA receptor expression/ degradation after blockade of  $\Delta$ FosB in the NTS during seven days of CIH.
8. AMPA receptor trafficking measurement by brefeldin A after blockade of  $\Delta$ FosB in the NTS during seven days of CIH.

9. AMPA receptor post-transcriptional modulations such as phosphorylation after blockade of  $\Delta$ FosB in the NTS during seven days of CIH.

10. Calcium imaging in arterial chemoreceptor second order NTS neurons infected by AAV-GFP- $\Delta$ JunD vector after seven days of CIH.

## CHAPTER V

### GENERAL DISCUSSION

In chapter II studies were conducted to examine the effect of NTS  $\Delta$ FosB blockade on the sustained hypertension induced during CIH in adult male Sprague-Dawley rats. NTS  $\Delta$ FosB blockade attenuated CIH induced hypertension. There was also a moderate reduction in the respiratory frequency during normoxic dark time in the CIH compared with sham group.  $\Delta$ FosB immunoreactivity in downstream sites of the NTS in arterial chemoreflex pathway like PVN was significantly reduced after NTS  $\Delta$ FosB inhibition, but no significant difference was observed in RVLM. In caudal ventro-lateral medulla (CVLM), the number of  $\Delta$ FosB was not affected by functional  $\Delta$ FosB blockade in NTS. Although the result of RVLM is not what was anticipated, neurons from other regions besides NTS project to RVLM and might have been activated during CIH (5, 9). CIH activating NTS neurons alone maybe not sufficient to drive transcriptional activation of the RVLM and other neurons might participate in the regulation. Additionally, the AAV did not infect all NTS neurons, so non viral-infected neurons may still project and regulate RVLM. CIH could increase  $\Delta$ FosB expression in NTS non-infected neurons which could activate  $\Delta$ FosB expression in RVLM. RVLM neurons could directly increase levels of FosB/ $\Delta$ FosB immunoreactivity in response to tissue hypoxia during CIH (9). Therefore, FosB/ $\Delta$ FosB immunoreactivity in RVLM might not decrease after NTS  $\Delta$ FosB blocking, or NTS  $\Delta$ FosB blocking decreases transcriptional activity of RVLM but the effect was not powerful enough to counter other RVLM excitation effects. Another explanation might be that the RVLM

is not involved in regulation of CIH associated hypertension through  $\Delta$ FosB. Other transcription factors might play a role in RVLM for CIH hypertension. Preliminary data from Dr. Glenn Toney's group found that dominant negative inhibition of  $\Delta$ FosB in RVLM cannot attenuate enhanced MAP induced by CIH (unpublished observation). The PVN might be the main CNS region that regulates CIH hypertension by the function of NTS  $\Delta$ FosB. Interestingly, our data here showed a little bit increase of  $\Delta$ FosB expression in RVLM after NTS  $\Delta$ FosB blockade, although not significantly different from sham control. Also a mild increase of  $\Delta$ FosB expression in CVLM was observed although not significant from sham control. Since the central part of baroreflex pathway includes CVLM and RVLM, this increase in  $\Delta$ FosB might occur in neurons responding to baroreflex, and the activated baroreflex could attenuate increased MAP induced by activated arterial chemoreflex during CIH.

To future investigate the mechanisms behind the role of NTS  $\Delta$ FosB in CIH induced hypertension, we studied  $\Delta$ FosB immunoreactivity in different durations of CIH exposure. Understanding the time course of  $\Delta$ FosB development could provide some hint about from what time point  $\Delta$ FosB might exert consequent cardiovascular regulatory functions. Results show that NTS  $\Delta$ FosB immunoreactivity increased from one day CIH to seven days CIH compared with normoxic control. One day normoxic recovery after seven days CIH was not significantly different from normoxic control. This result is concomitant with our time course of development of hypertension after seven days CIH. It shows that from the first CIH day, MAP started to increase and this increase lasted the entire seven days of CIH as well as the first day of recovery after the seven days CIH. By the first recovery day  $\Delta$ FosB expression had returned to control level, therefore  $\Delta$ FosB induces neuronal adaptive plasticity that persists in its absence.

In the caudal NTS, the time course of  $\Delta$ FosB immunoreactivity is consistent with the MAP response, while in the sub-postremal NTS,  $\Delta$ FosB immunoreactivity returned to control by 7 days CIH. There might be an adaptive process occurring in sub-postremal NTS. Sub-postremal NTS receives baroreceptor afferents input (1, 2), and activation of chemoreflex modulates baroreflex control of SNA (11). Additionally, a resetting of baroreflex control of renal SNA after 7 days of CIH was observed by Yamamoto et al (21). Therefore, we speculate that there is less baroreflex activation induced by tonic activation of the chemoreflex after 7 days of CIH. The low level of  $\Delta$ FosB expression after 7 days CIH in sub-postremal NTS could be an indicator of baroreflex resetting. Caudal NTS is mainly in charge of chemoreflex, 7 days of CIH activates chemoreflex, so there is more  $\Delta$ FosB presence in 7 days of CIH group in caudal NTS. Both augmented chemoreflex and attenuated baroreflex contribute to enhanced sympathetic activity by CIH.

Based on the time course of development in NTS  $\Delta$ FosB immunoreactivity, experiments were performed to study the time course of changes in glutamate transmission in NTS. Consistent with the  $\Delta$ FosB expression time course study, from one day to the whole seven days CIH, spontaneous glutamate transmission was elevated. One day recovery still showed elevated glutamate transmission as seen in CIH conditions. Combined with changes in MAP and NTS  $\Delta$ FosB expression during the seven days CIH treatment, along with changes in arterial chemoreceptor glutamate transmission, we believe there is a relationship between NTS  $\Delta$ FosB and CIH induced hypertension. Therefore, an AAV expressing dominant negative construct  $\Delta$ JunD was injected into NTS to block NTS  $\Delta$ FosB transcriptional activity, and then glutamatergic transmission was measured to determine the neuronal effects of NTS  $\Delta$ FosB inhibition. The results showed a moderate attenuation of CIH enhanced mEPSC amplitude after

$\Delta$ FosB inhibition, and an increase in mEPSC amplitude under normoxia after  $\Delta$ FosB overexpressing virus was injected into NTS.

$\Delta$ FosB overexpression in the nucleus accumbens (NAc) increased AMPA receptor subunit GluR2 levels, and this was associated with enhanced drug and natural reward (13-17, 20).

Changes of AMPA receptor expression warrants further investigation to address the molecular basis for the elevation of amplitude in mEPSCs observed after CIH. As  $\Delta$ FosB enhances GluR2 expression in rewarding pathway, we are interested in elucidating whether  $\Delta$ FosB in the NTS plays the similar role, so we applied western blot to measure expression of GluR2 in dominant negative group and sham group. We detected that in both the caudal and sub-postremal NTS, GluR2 levels were not significantly different after NTS  $\Delta$ FosB inhibition (unpublished observation). It is possible that unlike in the NAc, other factors might affect the transcriptional effect of  $\Delta$ FosB to target gene *glur2* in the NTS. We used the whole NTS region for western blot, without discriminating cell phenotypes, so it is possible that cells that do not receive input from arterial chemoreceptor and/ or non-affected by dominant negative antagonist injection might be included in this study. Furthermore, there is a possibility that in the NTS, membrane GluR2 expression decreased after  $\Delta$ FosB inhibition, but GluR2 phosphorylation induced by other factors caused AMPA receptor internalization (8). We used the whole NTS punches for western blot analysis, and both membrane and cytosolic fractions of GluR2 were counted, so the overall quantity of GluR2 did not change after  $\Delta$ FosB inhibition is not surprising. To better understand mechanisms for increase in mEPSC amplitude, in addition to AMPA receptor density, AMPA receptor sensitivity could be addressed. Post-transcriptional modulation such as phosphorylation could alter the sensitivity of AMPA receptor. Additionally, alterations in trafficking of AMPA receptor also could affect post- synaptic mechanisms for spontaneous glutamate transmission.

Our finding of weakened respiratory frequency following  $\Delta$ FosB inhibition in dark phase was interesting. There might be respiratory-sympathetic interactions that contribute to CIH-induced hypertension by increased respiratory drive to sympathoexcitatory neurons in the brain stem (12). Yamamoto et al. found that in acute intermittent hypoxia (AIH), there is a persistent increase in both phrenic and splanchnic sympathetic nerve activities in rats which is termed as long term facilitation (LTF) (21). They assumed that glutamatergic transmission plays a role in this LTF since CIH alters glutamatergic control of sympathetic and respiratory activities in the commissural NTS of rats (4). Based on our evidence that  $\Delta$ FosB mediates arterial chemoreceptor glutamate synaptic transmission in NTS under CIH, we can speculate that blocking  $\Delta$ FosB reduces glutamate transmission and thereby dampens phrenic nerve responses to CIH, leading to a reduced respiratory frequency.

Furthermore, function of corticosterone on glutamatergic transmission in arterial chemoreceptor NTS second order neurons has been studied by our group. CIH sensitizes HPA axis reactivity to stress (10) and increases plasma concentration of corticosterone (22). Corticosterone in the hindbrain contributes to enhanced arterial pressure in response to acute stress (18, 19). NTS catecholaminergic neurons express glucocorticoid receptors (6, 7) and project to PVN to activate Hypothalamo-pituitary adrenal (HPA) axis and knock-down of TH in NTS reduces CIH hypertension (3). CIH might activate the HPA axis to increase circulating corticosterone which binds to NTS glucocorticoid receptors to further augment neuronal responses to chemoreceptor activation. We have recorded the responses of arterial chemoreceptor NTS second order neurons to exogenous applied corticosterone and the amplitude of mEPSCs was significantly increased compared with non-corticosterone treatment, and this occurred at least 20 minutes after corticosterone application, indicating a delayed effect. Corticosterone did not change the

frequency of mEPSCs (Wu, Fan and Mifflin, unpublished observation, referred to appendix). Therefore, corticosterone could increase the discharge of NTS neurons involved in arterial chemoreflex pathway which might augment signaling to the downstream sympatho-excitatory regions to increase SND, resulting in neurogenic hypertension. Both catecholaminergic and non-catecholaminergic neurons could be the excited second order neurons. Interestingly, exogenous corticosterone had a much different effect in rats exposed to CIH. It did not significantly increase the amplitude or frequency of mEPSCs in the CIH exposed rats. In sum, in normoxic rats corticosterone induces a delayed post-synaptic enhancement of AMPA receptor mediated responses. In rats exposed to CIH, corticosterone does not induce any further post-synaptic increase in AMPA current or changes in the probability of glutamate synaptic release (Wu, Fan, and Mifflin, unpublished observation, referred to appendix). It is possible that under CIH, the increased circulating corticosterone saturates glucocorticoid receptors on NTS neurons, exogenous corticosterone could not be able to take further action, so the increased mEPSCs induced by CIH were not altered by bath applied additional corticosterone.

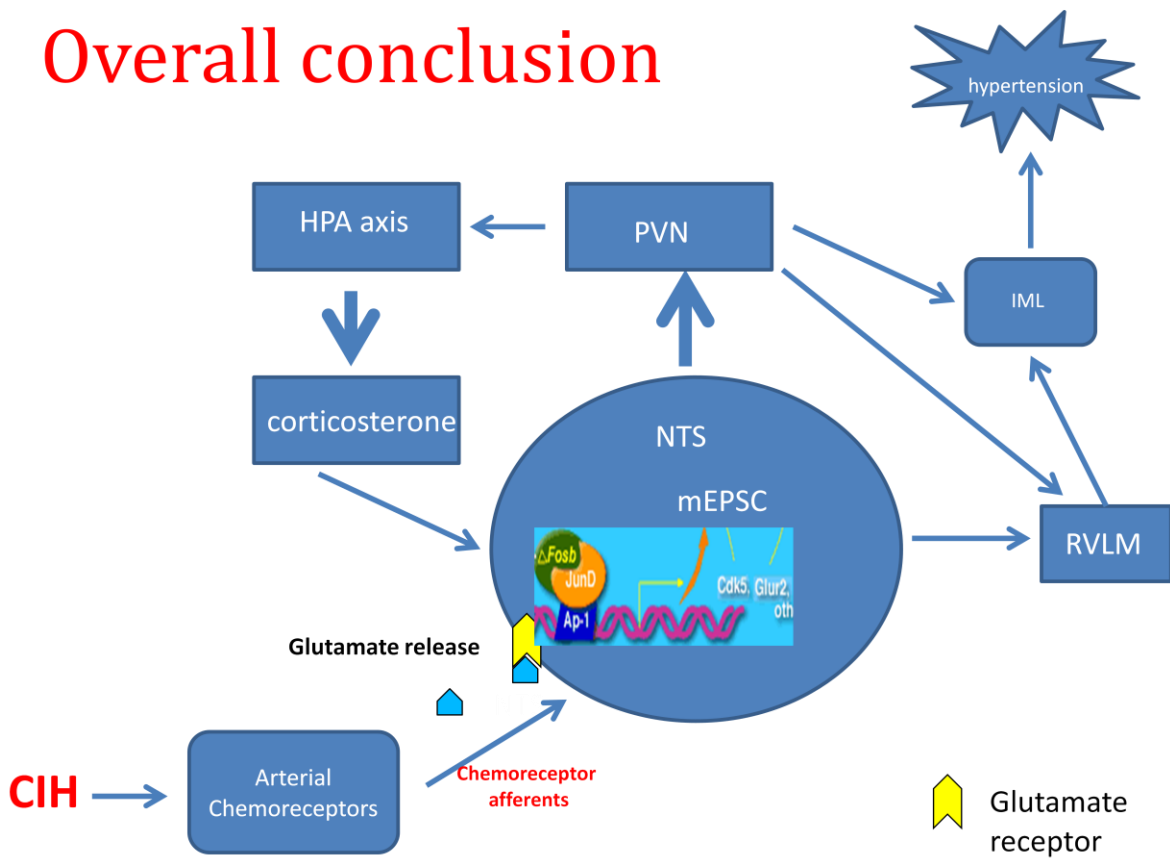
Based on these results, I propose the model shown below. Systemic hypoxia during CIH activates the arterial chemoreceptors and chemoreceptor afferents release glutamate on the second order NTS neurons. The released glutamate acts through AMPA receptors to cause an increased discharge of these neurons. Increased discharge, tissue hypoxia and/ or other factors induce transcription factor  $\Delta$ FosB and which further augments increased excitatory drive from these NTS neurons to their respective downstream sympatho-excitatory sites like PVN to activate IML of spinal cord to increase SND, resulting in hypertension. CIH induced hypertension could also result from increased excitatory drive from the arterial chemoreceptor second order NTS neurons to PVN to activate the HPA axis leading to increased corticosterone

release (10, 18, 19, 22), which could act back on the second order NTS neurons through glucocorticoid receptors to further augment neuronal responses to chemoreceptor activation and form a positive feedback loop. Through these pathways,  $\Delta$ FosB could play a role in sustained hypertension during CIH.

### **Clinical significance**

OSA, as the most common type of sleep apnea, represents a crucial disease burden to the global healthcare systems. Given the associations of OSA with cardiovascular diseases, especially the secondary resistant hypertension, the time has come to determine the underlying mechanisms that lead to this high mortality disease. The studies in this dissertation provide many new avenues for research into OSA associated hypertension. Addressing these mechanisms may provide novel therapeutic targets to OSA and OSA-related pathologies.

# Overall conclusion



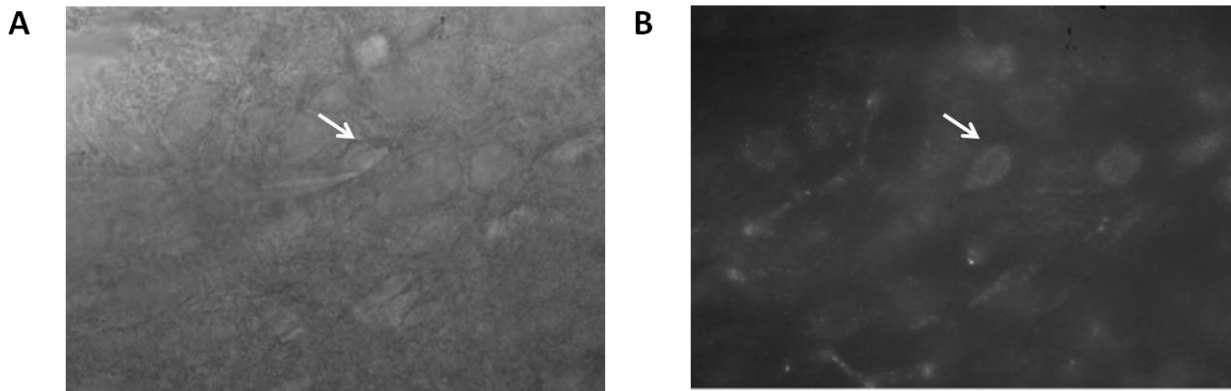
## **Reference**

1. **Accorsi-Mendonca D and Machado BH.** Synaptic transmission of baro- and chemoreceptors afferents in the NTS second order neurons. *Auton Neurosci* 175: 3-8.
2. **Andresen MC and Kunze DL.** Nucleus tractus solitarius--gateway to neural circulatory control. *Annu Rev Physiol* 56: 93-116, 1994.
3. **Bathina CS, Rajulapati A, Franzke M, Yamamoto K, Cunningham JT, and Mifflin S.** Knockdown of tyrosine hydroxylase in the nucleus of the solitary tract reduces elevated blood pressure during chronic intermittent hypoxia. *Am J Physiol Regul Integr Comp Physiol* 305: R1031-1039.
4. **Costa-Silva JH, Zoccal DB, and Machado BH.** Chronic intermittent hypoxia alters glutamatergic control of sympathetic and respiratory activities in the commissural NTS of rats. *Am J Physiol Regul Integr Comp Physiol* 302: R785-793.
5. **Cunningham JT, Knight WD, Mifflin SW, and Nestler EJ.** An Essential role for DeltaFosB in the median preoptic nucleus in the sustained hypertensive effects of chronic intermittent hypoxia. *Hypertension* 60: 179-187.
6. **Fuxe K, Cintra A, Agnati LF, Harfstrand A, Wikstrom AC, Okret S, Zoli M, Miller LS, Greene JL, and Gustafsson JA.** Studies on the cellular localization and distribution of glucocorticoid receptor and estrogen receptor immunoreactivity in the central nervous system of the rat and their relationship to the monoaminergic and peptidergic neurons of the brain. *J Steroid Biochem* 27: 159-170, 1987.
7. **Harfstrand A, Fuxe K, Cintra A, Agnati LF, Zini I, Wikstrom AC, Okret S, Yu ZY, Goldstein M, Steinbusch H, and et al.** Glucocorticoid receptor immunoreactivity in monoaminergic neurons of rat brain. *Proc Natl Acad Sci U S A* 83: 9779-9783, 1986.

8. **Jiang J, Suppiramaniam V, and Wooten MW.** Posttranslational modifications and receptor-associated proteins in AMPA receptor trafficking and synaptic plasticity. *Neurosignals* 15: 266-282, 2006.
9. **Knight WD, Little JT, Carreno FR, Toney GM, Mifflin SW, and Cunningham JT.** Chronic intermittent hypoxia increases blood pressure and expression of FosB/DeltaFosB in central autonomic regions. *Am J Physiol Regul Integr Comp Physiol* 301: R131-139.
10. **Ma S, Mifflin SW, Cunningham JT, and Morilak DA.** Chronic intermittent hypoxia sensitizes acute hypothalamic-pituitary-adrenal stress reactivity and Fos induction in the rat locus coeruleus in response to subsequent immobilization stress. *Neuroscience* 154: 1639-1647, 2008.
11. **Malpas SC, Bendle RD, Head GA, and Ricketts JH.** Frequency and amplitude of sympathetic discharges by baroreflexes during hypoxia in conscious rabbits. *Am J Physiol* 271: H2563-2574, 1996.
12. **Moraes DJ, Zoccal DB, and Machado BH.** Medullary respiratory network drives sympathetic overactivity and hypertension in rats submitted to chronic intermittent hypoxia. *Hypertension* 60: 1374-1380.
13. **Nestler EJ.** Is there a common molecular pathway for addiction? *Nat Neurosci* 8: 1445-1449, 2005.
14. **Nestler EJ.** Molecular basis of long-term plasticity underlying addiction. *Nat Rev Neurosci* 2: 119-128, 2001.
15. **Nestler EJ.** Molecular neurobiology of addiction. *Am J Addict* 10: 201-217, 2001.
16. **Nestler EJ.** Review. Transcriptional mechanisms of addiction: role of DeltaFosB. *Philos Trans R Soc Lond B Biol Sci* 363: 3245-3255, 2008.

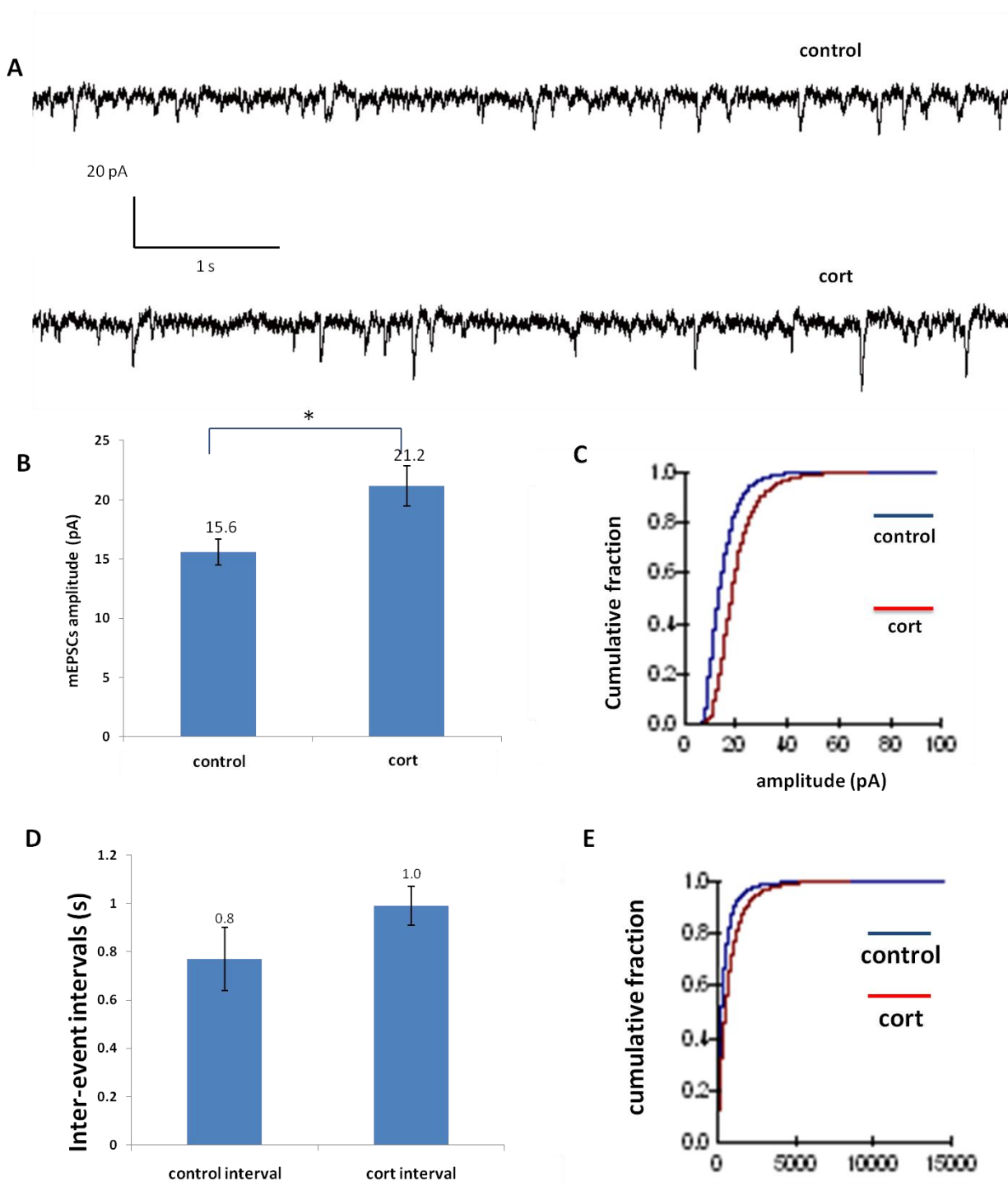
17. **Nestler EJ, Barrot M, and Self DW.** DeltaFosB: a sustained molecular switch for addiction. *Proc Natl Acad Sci U S A* 98: 11042-11046, 2001.
18. **Scheuer DA, Bechtold AG, Shank SS, and Akana SF.** Glucocorticoids act in the dorsal hindbrain to increase arterial pressure. *Am J Physiol Heart Circ Physiol* 286: H458-467, 2004.
19. **Scheuer DA, Bechtold AG, and Vernon KA.** Chronic activation of dorsal hindbrain corticosteroid receptors augments the arterial pressure response to acute stress. *Hypertension* 49: 127-133, 2007.
20. **Vialou V, Robison AJ, Laplant QC, Covington HE, 3rd, Dietz DM, Ohnishi YN, Mouzon E, Rush AJ, 3rd, Watts EL, Wallace DL, Iniguez SD, Ohnishi YH, Steiner MA, Warren BL, Krishnan V, Bolanos CA, Neve RL, Ghose S, Berton O, Tamminga CA, and Nestler EJ.** DeltaFosB in brain reward circuits mediates resilience to stress and antidepressant responses. *Nat Neurosci* 13: 745-752.
21. **Yamamoto K, Eubank W, Franzke M, and Mifflin S.** Resetting of the sympathetic baroreflex is associated with the onset of hypertension during chronic intermittent hypoxia. *Auton Neurosci* 173: 22-27.
22. **Zoccal DB, Bonagamba LG, Antunes-Rodrigues J, and Machado BH.** Plasma corticosterone levels is elevated in rats submitted to chronic intermittent hypoxia. *Auton Neurosci* 134: 115-117, 2007.

## APPENDIX



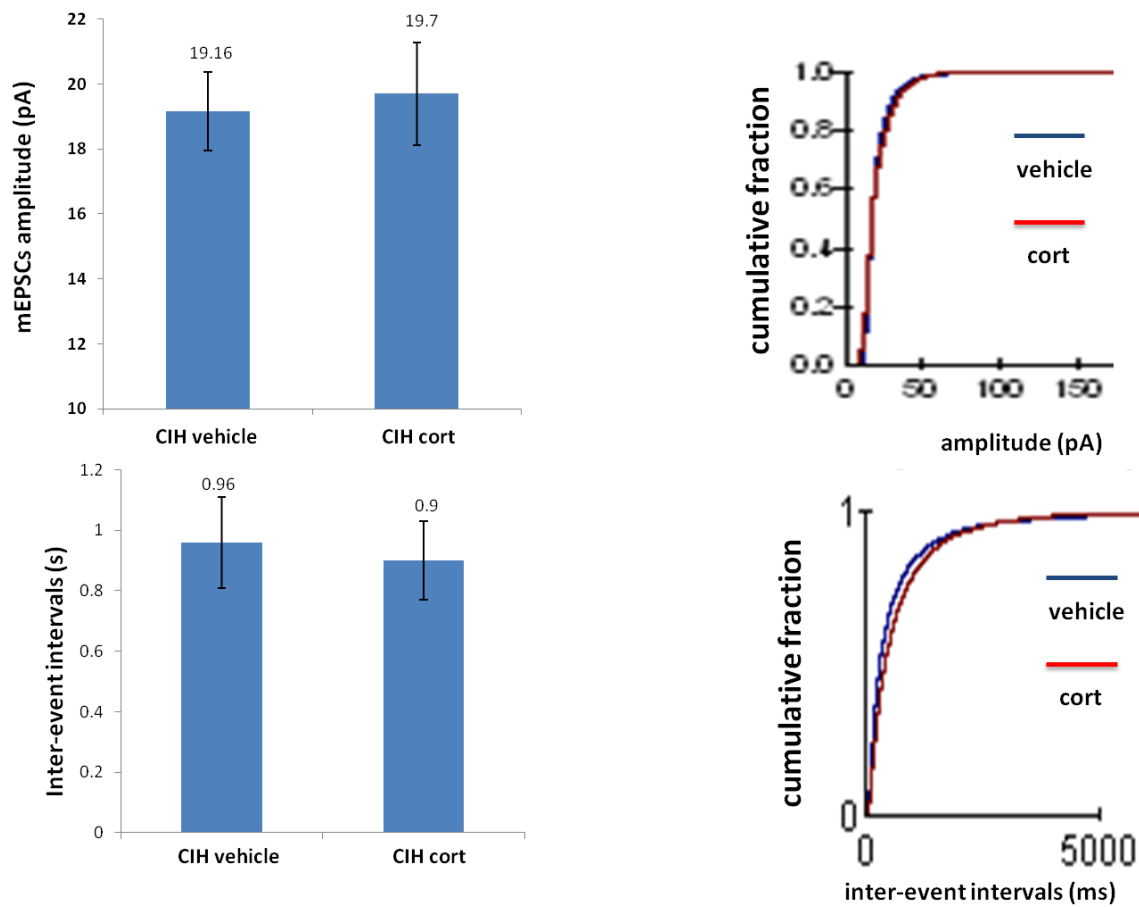
**Figure 1**

Figure 1. Representative digital images of NTS slice under (A) infrared differential contrast, (B) fluorescence. The arrow points to the neuron patched by a pipette and exhibits DiA immunofluorescence.



**Figure 2**

Figure 2. Effect of corticosterone on mEPSCs. A. raw traces of a neuron from a control slice and a neuron from a corticosterone treated slice. B. compared with control rats (n=12), there is an increase in amplitude of mEPSCs by corticosterone (n=10). C. cumulative frequency histogram shows a marked shift toward larger amplitude mEPSCs after corticosterone treatment. D. E. no significant difference in the frequency of mEPSCs between control and corticosterone treatment. All data were collected in the presence of the sodium channel blocker TTX (0.5  $\mu$ M) and GABA<sub>A</sub> receptor antagonist gabazine (25  $\mu$ M).



**Figure 3**

Figure 3. Combined effect of CIH and corticosterone on mEPSCs. No significant difference both in the amplitude and in the frequency of mEPSCs when compared CIH+vehicle (n=10) and CIH+corticosterone groups (n=12).